MOLECULAR AND CELLULAR BIOLOGY, Apr. 1991, p. 2133–2148
0270-7306/91/042133-16$02.00/0

Vol. 11, No. 4

The SIT4 Protein Phosphatase Functions in Late G_1 for Progression into S Phase

ANN SUTTON, DAVID IMMANUEL,† AND KIM T. ARNDT*

Cold Spring Harbor Laboratory, P.O. Box 100, Cold Spring Harbor, New York 11724

Received 15 November 1990/Accepted 24 January 1991

***Saccharomyces cerevisiae* strains containing temperature-sensitive mutations in the *SIT4* protein phosphatase arrest in late G_1 at the nonpermissive temperature. Order-of-function analysis shows that SIT4 is required in late G_1 for progression into S phase. While the levels of SIT4 do not change in the cell cycle, SIT4 associates with two high-molecular-weight phosphoproteins in a cell-cycle-dependent fashion. In addition, we have identified a polymorphic gene, *SSD1*, that in some versions can suppress the lethality due to a deletion of *SIT4* and can also partially suppress the phenotypic defects due to a null mutation in *BCY1*. The SSD1 protein is implicated in G_1 control and has a region of similarity to the dis3 protein of *Schizosaccharomyces pombe*. We have also identified a gene, *PPH2α*, that in high copy number can partially suppress the growth defect of *sit4* strains. The *PPH2α* gene encodes a predicted protein that is 80% identical to the catalytic domain of mammalian type 2A protein phosphatases but also has an acidic amino-terminal extension not present in other phosphatases.**

Progression through the eukaryotic cell cycle requires that many diverse processes be regulated in a precise temporal program. Current evidence indicates the existence of two major control points in the cell cycle: one at G_1/S which regulates initiation of DNA replication and one at G_2/M which regulates entry into mitosis. The requirement of protein kinases at both control points has been well established (2, 7, 18, 23, 39). However, for continued progression through the cell cycle, proteins that are phosphorylated by these kinases must be either degraded and resynthesized in the unphosphorylated form or dephosphorylated by protein phosphatases (PPases). Therefore, one proposed role of PPases is to reset a given protein kinase substrate to the nonphosphorylated form. In this scheme, the phosphorylation step is regulatory: a protein kinase that is precisely regulated in the cell cycle phosphorylates a substrate(s) for a given cell cycle event. However, it is also possible that it is the dephosphorylation step that regulates a cell cycle event. In this scheme, one might expect the PPase to be regulated in the cell cycle.

Four major classes of serine or threonine PPases from mammals are known (11). Type 1 PPases preferentially dephosphorylate the β subunit of phosphorylase kinase and are sensitive to inhibition by nanomolar concentrations of inhibitors I1 and I2 and by micromolar concentrations of okadaic acid. The three classes of type 2 PPases preferentially dephosphorylate the α subunit of phosphorylase kinase. Type 2A PPases require no added cations for activity and are sensitive to nanomolar concentrations of okadaic acid. The catalytic subunit of type 2A PPases is about 50% identical at the amino acid level to the catalytic subunit of type 1 PPases. Type 2B PPases (also called calcineurin) require Ca^{2+} for activity and have a region of 110 amino acids in the catalytic subunit that is about 33% identical to the corresponding regions of the catalytic subunits of type 1 and type 2A PPases. Type 2C PPases require Mg^{2+} for activity and have no amino acid sequence similarity to type 1 or type 2A PPases.

Very little is known about the role of PPases in the cell cycle. Recently, type 1 PPases have been implicated as being required for progression through mitosis. Cold-sensitive mutations in the *Schizosaccharomyces pombe dis2* gene (=*bws1* [9]), which encodes a predicted type 1 PPase, arrest in mitosis at the nonpermissive temperature (27). Also, a temperature-sensitive mutation in the *Aspergillus nidulans bimG* gene, which also encodes a predicted type 1 PPase, causes a mitotic block at the nonpermissive temperature (16). In *Drosophila melanogaster*, mutations in one of the four genes which encode type I PPase isozymes result in abnormal mitosis, chromosome segregation, and chromosome condensation (5).

The SIT4 PPase was originally identified in *Saccharomyces cerevisiae* by mutations (*sit4*) that restore transcription to the *HIS4* gene in the absence of GCN4, BAS1, and BAS2 (4). GCN4, BAS1, and BAS2 are *trans*-acting DNA binding factors that are normally required for *HIS4* transcription. These *sit4* mutations cause alterations in the transcription of many diverse genes in addition to *HIS4*. Strains containing transcriptional suppressor *sit4* mutations grow very slowly, are temperature sensitive for growth, and do not grow on nonfermentable carbon sources (4). The *SIT4* gene encodes a predicted protein of 35.5 kDa that is 55% identical to the catalytic subunit of mammalian type 2A PPases and 40% identical to the catalytic subunit of mammalian type 1 PPases (4).

In this report, we show that the SIT4 PPase functions in late G_1 for progression into S phase. In addition, we identify a new gene, *SSD1*, that is implicated in G_1 control. Certain alleles of *SSD1* can suppress the lethality due to a deletion of *SIT4*. Biochemical analysis of SIT4 shows that SIT4 associates with two high-molecular-weight proteins, p155 and p190, and that this association is cell cycle dependent.

MATERIALS AND METHODS

Strains and media. Table 1 shows the genotypes of yeast strains used in this study. YPD, GNA, YPGE, and SC are as described previously (4). All carbon sources were used at a

* Corresponding author.
† Present address: Wesleyan University, Box 4468, Middletown, CT 06457.

TABLE 1. Yeast strains

Strain	Background[a]	Genotype	Source or reference
L3110		*MATa gcn4-2 bas1-2 bas2-2 ura3-52 SSD1-v2*	4
AY910	L	*MATa*(YEp24)	4
AY953	L	*MATa*(*SIT4* on Yep24)	4
S/A225-23-5	L	*MATa sit4-36*	4
S/A225-26-3	L	*MATa sit4-37*	4
S/A225-29-3	L	*MATa sit4-39*	4
W303		*MATa ade2-1 his3-11,15 leu2-3,112 can1-100 ura3-1 trp1-1 ssd1-d2*	R. Rothstein
CY49	W	*MATa sit4-(SIT4* on YCp50)	This study
CY93	W	*MATa sit4-1(sit4-102* on *LEU2*/cen plasmid)	This study
CY105	W	*MATα sit4-1(SIT4* on *LEU2*/cen plasmid)	This study
CY146	W	*MATa sit4-2(sit4-102* on *LEU2*/cen plasmid)	This study
CY160	W	*MATa sit4-2(SIT4* on YCp50)	This study
CY198	W	*MATa sit4-2(SIT4* on YEp24)	This study
CY199	W	*MATa sit4-2(SIT4* on *LEU2*/cen plasmid)	This study
CY200	W	*MATa sit4-2*(NH_2-tagged *SIT4* on *LEU2*/cen plasmid)	This study
CY202	W	*MATa sit4-2*(COOH-tagged *SIT4* on *LEU2*/cen plasmid)	This study
CY249	W	*MATα sit4-2(sit4-102* on YCp50)	This study
CY798	W	*MATa ssd1::LEU2*	This study
CY823	W	*MATα*(YCp50)	This study
CY825	W	*MATα(SSD1-v1* on YCp50)	This study
CY827	W	*MATα(SSD1-v1* on YEp24)	This study
CY845	W	*MATa pGAL:SIT4*	This study
CY81		*MATα cdc28-13 ura3-52 leu2-3 met8*	Arndt laboratory strain
CY182		*MATa his3Δ200 leu2-3 ura3-52 lys2 SSD1-v1*	Arndt laboratory strain
CY240		*MATa cdc28-13 his3-11,15 leu2-11,113 lys2^0 tyr1^0 trp1-1 ade2-1*	Arndt laboratory strain
CY248		*MATa sit4-2 his3 leu2-3 ura3 SSD1-v1*	Obtained from cross of CY146 and CY182
CY279		*MATα sit4-2 leu2-3 trp1-1 his3 ura3 SSD1-v1*	Obtained from cross of CY146 and CY182
CY738		*MATa sit4-2 his3 leu2 trp1 lys2-801 ura3 ade2 ssd1-d1* (*sit4-102* on YCp50)	Obtained from cross of YP6D and CY249
YP6D		*MATa his3 leu2 trp1 lys2-801 ura3 ade2 ssd1-d1*	P. Heiter
S288C		*MATα gal2 SSD1-v1*	F. Winston
T25-1		*MATa cdc25-1 leu2 his3 trp1*	M. Wigler
MDMy256		*MATa cdc28-13 met8 his7 tyr1^0*	M. Mendenhall

[a] Strains in the L series are isogenic to strain L3110 except as indicated; strains in the W series are isogenic to strain W303 except as indicated.

final concentration of 2% except for GNA, which contained 5% glucose.

Phenotypic analyses. Qualitative glycogen levels of patches of cells were determined by inverting plates over iodine crystals for 3 to 5 min. Heat shock assays were done by replica plating cells to plates prewarmed at 55°C and incubating at 55°C for 2 min. Plates were then incubated for 2 days at 30°C.

Order-of-function mapping. Cultures of cells (2.5×10^6 cells per ml) were treated with 80 μg (for T25-1 and MDMy256) or 160 μg (for CY738 and YP6D) of synthetic α factor per ml in YPD and incubated for 3.5 h at the permissive temperature. This amount of α factor was determined by titration to be sufficient to arrest 98% of the cells but to allow recovery of each strain in about 30 min after filtering. Cells were filtered, washed twice with YPD, and resuspended in YPD. At 5-min intervals after release from α factor, aliquots of the strains were shifted to the nonpermissive temperature (37°C) and monitored for an additional 4.5 h. For the reciprocal analysis, asynchronous cultures were first placed at 37°C for 4.5 h and then shifted to the permissive temperature for 4 h following addition of α factor. Budding of cells was monitored microscopically following a brief sonication to disrupt aggregates.

Immunofluorescence. 4′, - 6′ - Diamidino - 2 - phenylindole (DAPI) staining and immunological staining of cells for tubulin was carried out as described previously (20). For analysis of arrested cells, exponentially growing cultures were shifted to the nonpermissive temperature for 4.5 h before fixation with formaldehyde. For tubulin staining, the 1^0 antibody was anti-tubulin antibody YOL/34 (Sera Lab) and the 2^0 antibody was goat anti-rat immunoglobulin G-fluorescein isothiocyanate (Boehringer Mannheim). For SIT4 localization, the 1^0 antibody was affinity-purified anti-SIT4 peptide antibody and the 2^0 antibody was goat anti-rabbit immunoglobulin G-fluorescein isothiocyanate (Boehringer Mannheim). Cells were viewed with a Zeiss Axiophot microscope with a 100× objective. Kodax Tri-X Pan 400 film was used for photography.

Preparation of cellular extracts and Western immunoblotting. Exponentially growing cells were harvested by centrifugation and washed with ice-cold lysis buffer (100 mM Tris-HCl, pH 7.5, 200 mM NaCl, 1 mM EDTA, 5% glycerol, 0.5 mM dithiothreitol). Cells were resuspended in 300 μl of lysis buffer (containing 1 mM phenylmethylsulfonyl fluoride and 1.25 μg each of leupeptin, antipain, chymostatin, and pepstatin per ml [Sigma]) and lysed by vortexing four times in the presence of glass beads for 15-s intervals. An additional 350 μl of lysis buffer containing protease inhibitors was added, and the cells were vortexed again for 15 s. The liquid was pipetted from the glass beads and centrifuged at $16,000 \times g$ for 8 min to remove cell debris. An equal volume

of 2× gel sample buffer (32) was added to the extracts, which were then heated for 5 min at 95°C, centrifuged for 3 min at 16,000 × *g* to remove aggregates, and electrophoresed through sodium dodecyl sulfate-polyacrylamide gels (22). The separated proteins were analyzed by Western immunoblotting (37).

Subcellular fractionation. Fractionation of strain CY199 (containing wild-type SIT4) was carried out as described previously (1) to obtain a pellet of crude nuclei and a postnuclear supernatant. Proteins were precipitated from the supernatant by addition of trichloroacetic acid (TCA) to 10%. The TCA precipitates and the nuclear pellet from equal numbers of cells were resuspended in 10 mM Tris (pH 7.4)–20 mM KCl. Equal volumes of 2× gel sample buffer were added, and the samples were heated to 95°C for 5 min. After centrifugation for 3 min at 16,000 × *g*, samples were fractionated on an 8% polyacrylamide gel and immunoblotted.

Preparation of labeled proteins and immunoprecipitation. For ^{35}S labeling of proteins, cells were grown in yeast nitrogen base (Difco) supplemented with the required amino acids at 0.1 μg/ml (except 0.2 μg/ml for leucine and adenine at 0.3 mM). When cells reached an A_{600} of about 0.4, they were centrifuged and resuspended in 10 ml of fresh medium at an A_{600} of 2.0 containing 0.25 mCi of [^{35}S]methionine (1,151 Ci/mmol; Du Pont). The cells were incubated for 75 min at 30°C before being harvested. For ^{32}P labeling of proteins, cells were grown in YPD which had been depleted of inorganic phosphate (YPD-PO_4 [3]). At an A_{600} of about 0.4, cells were centrifuged as described above and resuspended at an A_{600} of 2.0 in fresh YPD-PO_4 containing 0.8 mCi of $^{32}P_i$ (296 mBq/ml; Amersham). After being labeled for 70 min at 30°C, cells were harvested by centrifugation and washed twice in ice-cold H_2O and once in ice-cold lysis buffer. Cell extracts were prepared as described above. For the experiment in Fig. 6, the labeled cells were processed in lysis buffer which had been supplemented with 10 mM Na fluoride, 1 mM $NaPP_i$, and 1 mM Na vanadate.

For immunoprecipitation, 75 μl of an extract in lysis buffer (at 0.8 mg/ml of protein; determined by using the Bio-Rad protein assay) was incubated with 0.5 μl of monoclonal antibody (MAb) 12CA5 ascites (at 1.9 mg/ml of protein; determined by using the Bio-Rad protein assay) in a total volume of 100 μl. After 60 min at 0°C, aggregates were removed by centrifugation at 16,000 × *g* for 15 min. The supernatant was transferred to 50 μl of a suspension of protein A-Sepharose beads (Pharmacia; 100 mg/ml in RIPA buffer [50 mM Tris-HCl, pH 7.5, 200 mM NaCl, 1% Triton X-100, 0.5% Na deoxycholate, 0.1% sodium dodecyl sulfate]). The mixture was incubated with gentle rocking for 50 min at 4°C. The beads were washed four times with 75% lysis buffer–25% RIPA buffer (containing 1 mM phenylmethylsulfonyl fluoride) and then once with 50 mM Tris-HCl (pH 7.5)–50 mM NaCl. The beads were sucked dry and resuspended in 30 μl of 2× gel sample buffer, heated for 5 min at 95°C, and centrifuged at 16,000 × *g* for 3 min. The supernatant was subjected to electrophoresis on 8% polyacrylamide gels. For the experiment in Fig. 6, the beads for all samples were treated for 7 min on ice with 3.5 μg of RNase (Sigma) and 7 μg of DNase (Worthington) prior to the addition of sample buffer. Gels were treated with Amplify (Amersham) according to the instructions of the manufacturer. Competition with the hemagglutinin peptide (YPYDVPDYA) was done by incubation of 0.5 μl of MAb 12CA5 with 10 μg of peptide for 30 min at 0°C before addition to extracts.

Gel filtration chromatography. Gel filtration chromatography was carried out on Sephadex G200 columns equilibrated with 90% lysis buffer–10% RIPA buffer containing 1 mM phenylmethylsulfonyl fluoride. Cell extracts (0.6 ml, 1.2 mg/ml of protein in 90% lysis buffer–10% RIPA buffer containing 1 mM phenylmethylsulfonyl fluoride) prepared as described above were loaded onto the column and eluted in equilibration buffer. Fractions (0.8 ml) were collected and analyzed either by immunoprecipitation (for ^{35}S-labeled proteins) or by Western analysis. Immunoprecipitation was carried out as described above except that 0.5 μl of the MAb 12CA5 ascites (at 1.9 mg/ml of protein; determined by using the Bio-Rad protein assay) was added to the entire 0.8-ml fraction and 30 μl of the protein A-Sepharose bead suspension was used. For Western analysis, proteins were precipitated from each fraction by the addition of insulin to 100 μg/ml followed by the addition of TCA to 10% and incubation at 0°C for 30 min. Precipitates were collected by centrifugation, washed with 5% TCA, and resuspended in 2× gel sample buffer. The pH was neutralized by the addition of 2 M Tris-HCl (pH 9.0), and the samples were heated, centrifuged, and electrophoresed as described above. Western immunoblotting with anti-SIT4 peptide antibody was as described above except that the antibody used was not affinity purified. In order to control for the efficiency of recovery, 10 μl of an extract (0.5 mg/ml of protein) prepared from a strain which contains a deletion of *SIT4* and an epitope-tagged version of SIS1 was added to each fraction prior to TCA precipitation. The Western blots were first probed with the anti-SIT4 peptide antibody to detect the SIT4 protein. The blots were then probed with MAb 12CA5 ascites to detect the epitope-tagged SIS1 protein. The level of SIS1 did not vary more than 10% among lanes.

Centrifugal elutriation of cells. To obtain G_1 cells for gel filtration chromatography, 10^{10} cells from an exponentially growing culture were concentrated by centrifugation, resuspended in 50 mM Tris-HCl (pH 7.5)–50 mM NaCl at 4°C, and sonicated briefly to separate mother cells from completed daughter buds. Cells were then loaded into a Beckman JE-5.0 elutriator rotor at 4°C at a rotor speed of 2,800 rpm and a pump speed of 20 ml/min. Small unbudded cells were eluted by increasing the pump speed to 35 ml/min. The cells were washed once in lysis buffer, and extracts were prepared. To obtain S/G_2 cells, eluted G_1 cells were grown at 30°C until 90% of the cells had formed buds before the extracts were prepared.

Centrifugal elutriation was used to isolate ^{35}S-labeled cells from different stages of the cell cycle as follows. One hundred milliliters of an exponentially growing culture of strain CY202 was labeled for 75 min with 1.25 mCi of [^{35}S]methionine as for immunoprecipitations. Cells were harvested, washed twice, and resuspended in 50 mM Tris-HCl (pH 7.5)–50 mM NaCl at 4°C. After sonication, cells were loaded into the elutriator rotor. Fractions of cells from throughout the cycle were eluted at a constant pump speed of 35 ml/min by decreasing the centrifugation speed by 100 rpm for each fraction. Extracts were prepared and immunoprecipitations were carried out as described above. A small aliquot of each fraction was removed prior to cell lysis, and the DNA content was analyzed by flow cytometry as described previously (25).

Preparation of anti-SIT4 peptide antibodies. A 16-amino-acid peptide (MVSRGPDEWLETIKKC) corresponding to the amino terminus of SIT4 was coupled to keyhole limpet hemocyanin as described previously (19) and injected into rabbits. Affinity purification of the antiserum was by chromatography on a column containing the same SIT4 peptide

coupled to bovine serum albumin and immobilized on Reactigel (Pierce). After being rinsed, the purified antibodies were eluted from the column with 100 mM glycine (pH 2.5) and were dialyzed against phosphate-buffered saline.

Isolation and characterization of *SSD1*. A 809-bp *Eco*RI-*Bam*HI fragment containing the *GAL1* promoter was inserted into a unique *Hpa*I site created by oligonucleotide mutagenesis 12 bp upstream of the A of the ATG of the *SIT4* open reading frame. The oligonucleotide mutagenesis changed the *SIT4* upstream sequence from CAATAACA ATGGTA to CAATAACAATGGTATCTAGAGTTAACAC AATAACAAATGGTA (both the HpaI site and the *SIT4* ATG methionine start codon are underlined). The resulting *pGAL:SIT4* fragment was used to replace the chromosomal copy of *SIT4* in strain W303. The resulting strain, CY845, was viable when grown on galactose but inviable on glucose medium. CY845 was transformed to Ura$^+$ on SC-Ura galactose plates with a yeast genomic library in YCp50 (30). From a total of 50,000 transformants, two classes of plasmids were obtained which allowed growth of CY845 on glucose. Restriction enzyme analysis revealed that one class contained the *SIT4* gene. To prove that the second class contained the *SSD1* gene, we inserted a noncomplementing 1.7-kb *Bam*HI-*Eco*RI fragment of *SSD1* into the *URA3* plasmid, YIp5, and directed integration at the *SSD1* locus of CY279 (*SSD1-v1 sit4-2*) by homologous recombination (by cutting with *Bst*EII at −349 relative to the ATG of *SSD1*). The resulting strain, which has *URA3* tightly linked to *SSD1-v1*, was crossed to CY199 (*ssd1-d2 sit4-2 SIT4* on a *LEU2*/cen plasmid). The diploid was cured of the *LEU2*/cen plasmid containing the *SIT4* gene and then sporulated, and tetrads were dissected. All viable progeny which contained the deletion of *SIT4* (*sit4-2*) were Ura$^+$, demonstrating that viability in the absence of *SIT4* was completely linked to the *SSD1-v* gene.

The smallest complementing *SSD1-v1* fragment was inserted into pUC118 in both orientations and sequenced as described previously (34). Deletion analysis indicated that the single large open reading frame on this fragment encodes SSD1. The *SSD1* gene was placed on the yeast physical map to a position near *GCN2* on chromosome IV by L. Riles and M. Olsen (28a). They probed their overlapping set of yeast genomic clones with the *SSD1* gene. Meiotic mapping shows that the distance between *ssd1::LEU2* (see below) and *gcn2-284* is 3 centimorgans (cM) (63 parental ditype [PD], 4 tetratype [T], 0 nonparental ditype [NPD]), the distance between *ssd1::LEU2* and *lys4* is 25.4 cM (33 PD, 34 T, 0 NPD), and the distance between *lys4* and *gcn2-284* is 22.4 cM (37 PD, 30 T, 0 NPD). The segregation pattern of a three-point cross showed the gene order to be *LYS4 GCN2 SSD1*.

Two different chromosomal deletions of *SSD1* were prepared. One deletion, termed *ssd1::HIS3*, was created by replacing an *Eco*RI-*Xba*I fragment internal to the *SSD1* coding region with a 1.8-kb *Bam*HI fragment containing the *HIS3* gene. A fragment containing the *ssd1::HIS3* disruption was used to replace one chromosomal copy of *SSD1* in a W303 homozygous diploid. The *ssd1::HIS3/SSD1* diploid was sporulated, and the tetrads were dissected. All four progeny of each tetrad were viable and grew at the same rate. A second deletion, *ssd1::LEU2*, was created by replacing a *Bst*EII-*Eco*RI fragment of *SSD1* with a 2.2-kb *Sal*I-*Xho*I fragment containing the *LEU2* gene. Phenotypes of strains containing either *ssd1::HIS3* or *ssd1::LEU2* are identical.

Chromosomal deletion of *SIT4*. Two different chromosomal deletions of *SIT4* were prepared. One deletion, termed *sit4-2*, was prepared as follows. A DNA fragment in which almost the entire *SIT4* coding sequences (amino acids 4 to 308 deleted of 311 total) were replaced by a 1.8-kb *Bam*HI fragment containing the *HIS3* gene was used to replace one chromosomal copy of *SIT4* in a W303 diploid. The *sit4-2/SIT4* W303 diploid was sporulated, and the tetrads were dissected. No more than two colonies grew from any of the dissected tetrads, and no His$^+$ colonies were recovered. When the *sit4-2/SIT4* diploid was transformed with the wild-type *SIT4* gene on a *URA3*/cen plasmid, Ura$^+$ progeny were obtained that contained the chromosomal deletion of *SIT4*. However, these colonies could not grow in the absence of the plasmid containing the wild-type copy of the *SIT4* gene. A second deletion, *sit4-1*, was created by replacing a *Bgl*II-*Nru*I fragment with the 1.8-kb *Bam*HI fragment containing the *HIS3* gene. Phenotypes of strains containing either *sit4-1* or *sit4-2* are identical.

Isolation of *sit4-102*. The *SIT4* gene on a *LEU2*/cen plasmid was mutagenized with hydroxylamine as described previously (29). The mutagenized plasmid was transformed into strain CY160 which has a chromosomal deletion of *SIT4* and wild-type *SIT4* on a *URA3*/cen plasmid. Leu$^+$ transformants which had lost the *URA3*/cen plasmid were selected on 5-fluoro-orotic acid (8) and screened for temperature sensitivity. For one plasmid obtained, it was determined by subcloning that the temperature sensitivity it conferred resulted from a mutation in *SIT4* coding sequences.

Epitope tagging of SIT4. Duplex oligonucleotides encoding the epitope sequence YPYDVPDYA were placed into either the *Xba*I site of *SIT4* (for amino-terminal tag) or the *Nae*I site of *SIT4* (for carboxyl-terminal tag). Tagging at the amino terminus changes SIT4 from MVSRGP to MVSSYPYDVP DYASRGP. Tagging at the carboxyl terminus changes SIT4 from RAGYFLstop to RAGYPYDVPDYASGYFLstop. *ssd1-d2* strains containing either amino-terminally or carboxyl-terminally tagged SIT4 as the only source of SIT4 grow slightly more slowly (doubling time of 95 min for NH_2-tagged SIT4 and 84 min for COOH-tagged SIT4, in YPD) than strains containing wild-type SIT4 (doubling time of 70 min, in YPD).

Isolation and characterization of *PPH2α*. The *PPH2α* gene was isolated from a yeast genomic library in YEp24, a high-copy-number plasmid in *S. cerevisiae* (10). A 1.8-kb *Xba*I-*Sna*BI fragment of the original yeast insert gave full complementation (in high copy number) for partial suppression of the growth defect of strains containing transcriptional suppressor *sit4* mutations. This fragment was placed into pUC118 in both orientations and sequenced as described previously (34).

Oligonucleotide-directed mutagenesis was used to delete sequences of *PPH2α* corresponding to amino acids 35 to 375 (of 377 total) and replace them with a *Bgl*II site. The 1.8-kb *Bam*HI fragment of *HIS3* was inserted into this *Bgl*II site. This deletion allele, termed *pph2α-2*, was placed into the chromosome of a W303 diploid by homologous recombination. Haploid progeny that contained the chromosomal deletion of *PPH2α* were viable and grew at wild-type rates.

The *PPH2α* gene was placed on the yeast physical map on the left arm of chromosome IV by Riles and Olsen (28a) by probing their set of yeast clones with the *PPH2α* gene. A *URA3*-marked *PPH2α* locus was created by inserting the *PPH2α* gene into YIp5. The resulting plasmid was digested with *Sac*I (cuts within *PPH2α*) and transformed into W303 to direct integration at *PPH2α*. The correct integration was confirmed by Southern analysis. The *URA3*-marked *PPH2α* allele was used for meiotic mapping of *PPH2α*. *PPH2α* maps

16.7 cM from *cdc9-1* (54 PD, 27 T, 0 NPD) and 46 cM from *cdc2-1* (15 PD, 26 T, 4 NPD). The segregation pattern of a three-point-cross confirmed the gene order as *PPH2α CDC9 CDC2*.

The 5′ end of the *PPH2α* mRNA was mapped by using primer extension analysis (performed as in reference 24) of total yeast RNA with two different nonoverlapping primers. These two primers correspond to DNA sequences from 249 to 231 and from 339 to 321 of *PPH2α*. The 5′ ends of *PPH2α* mRNA predicted by both primers were in agreement.

Nucleotide sequence accession numbers. The GenBank accession number for *SSD1* is M60318. The GenBank accession number for *PPH2α* is M60317.

RESULTS

Arrest of *sit4* mutants in G_1 at the nonpermissive temperature. Strains containing *sit4* transcriptional suppressor mutations grow very slowly and are temperature sensitive for growth (4). When shifted to the nonpermissive temperature, strains containing *sit4* transcriptional suppressor mutations give a first-cycle arrest with greater than 85 to 90% unbudded cells. DAPI staining and staining for microtubules by indirect immunofluorescence show that the arrested cells are uninucleate and contain a single microtubule organizing center (*sit4-37* and *sit4-39*; Fig. 1). The microtubule organizing center is the yeast spindle pole body. The arrested cells have a 1*n* DNA content as determined by flow cytometer analysis. These results indicate that strains containing transcriptional suppressor mutations in *sit4* give a cell cycle arrest in G_1 at the nonpermissive temperature.

All of the *sit4* transcriptional suppressor mutations were obtained by selecting for a His^+ phenotype. To show that this G_1 arrest is not unique to the transcriptional suppressor alleles of *SIT4*, we sought to create new alleles of *SIT4* based only on a temperature-sensitive phenotype. The *SIT4* gene on a *LEU2*/cen vector was mutagenized with hydroxylamine and transformed into strain W303 (33) containing a chromosomal deletion of *SIT4* and the wild-type *SIT4* gene on a *URA3*/cen vector. Leu^+ transformants were cured of the *URA3*/cen vector (8) and screened for temperature-sensitive growth. From this screen, we obtained one allele, *sit4-102*, which gives relatively good growth at 30°C (doubling time = 114 min; doubling time of isogenic wild type = 70 min; in YPD) but no growth at the nonpermissive temperature.

When strains containing the *sit4-102* allele (in a *ssd1-d2*=W303 or in a *ssd1-d1* background; see below) are shifted to the nonpermissive temperature, 85 to 90% of the cells give a first-cycle arrest as large unbudded uninucleate cells with a single microtubule organizing center (Fig. 1). Arrested *sit4-102* cells (in a *ssd1-d1* background) have a 1*n* DNA content as determined by flow cytometry analysis. Electron microscopic analysis of serial sections of these arrested cells shows a single unduplicated spindle pole body. We could not determine whether the single spindle pole body had formed a satellite structure. In summary, the above results show that strains containing either *sit4-102* or *sit4* transcriptional suppressor mutations arrest in G_1 at the nonpermissive temperature.

SSD1*: a polymorphic gene that in some forms can permit strains with a deletion of *SIT4* to live.** A deletion of the *SIT4* gene (termed *sit4-2*), which replaces almost all of the *SIT4* coding sequences with the *HIS3* gene, was originally created in a diploid strain prepared from isogenic ***a and α W303 haploid strains. When *sit4-2*/*SIT4* W303 diploids are sporulated and the tetrads are dissected, the two *sit4-2* spores in each tetrad germinate but arrest as very large unbudded cells at the 8- to 16-cell stage. The *sit4-2*/*SIT4* diploid strain was then transformed with the wild-type *SIT4* gene on a *URA3*/cen plasmid and sporulated. Haploid *sit4-2* W303 strains containing the wild-type *SIT4* gene on the *URA3*/cen plasmid were obtained. These strains are not able to grow in the absence of the plasmid containing the wild-type *SIT4* gene. One of these strains was used to isolate the temperature-sensitive *sit4-102* allele as described above.

Surprisingly, when *sit4-2* W303 haploid strains containing the wild-type *SIT4* gene on a plasmid were crossed to other strain backgrounds, about one-half of the crosses yielded very slowly growing *sit4-2* haploid progeny that did not contain the plasmid with the wild-type *SIT4* gene (plasmids segregate independently during meiosis). Genetic analysis showed that the ability to grow very slowly (doubling time = about 200 min; doubling time of isogenic *SIT4* strain = 70 min; in YPD) in the absence of *SIT4* segregates as a single genetic locus, unlinked to *SIT4*. Also, the alleles of this locus that allow life in the absence of *SIT4* are dominant (with respect to viability) over the alleles that do not allow life in the absence of *SIT4*. We term this gene *SSD1*, for suppressor of SIT4 deletion. In order to isolate *SSD1*, we prepared strain CY845, a W303 haploid in which the chromosomal *SIT4* gene is under control of the *GAL1* promoter. This strain is viable when grown on galactose (*GAL1* promoter induced, *SIT4* expressed) but is inviable when grown on glucose (*GAL1* promoter repressed, *SIT4* not expressed). Strain CY845 was transformed to Ura^+ on galactose medium with a yeast genomic library in the *URA3* plasmid YCp50 (30). This library was prepared from strain S288C in which a deletion of *SIT4* is viable. Transformants were replica plated to glucose, and the library plasmid was recovered from colonies that were able to grow on glucose. This analysis gave two classes of plasmids. One class, which gave wild-type growth rates in strain CY845 grown on glucose medium, contained the *SIT4* gene. The second class, which gave very low growth rates in strain CY845 grown on glucose medium, contained the putative *SSD1* gene. Genetic analysis showed that the second class contained the authentic *SSD1* gene (see Materials and Methods). The *SSD1* gene maps to a previously unidentified genetic locus, 3 cM from *GCN2* (gene order: *LYS4 GCN2 SSD1 TRP4*) on chromosome IV (see Materials and Methods).

The *SSD1* gene encodes a predicted protein of 1,250 amino acids with a molecular mass of 140.0 kDa (Fig. 2A). SSD1 has no significant similarity to any protein in GenBank or EMBL (release no. 64). However, a computer search by Mark Goebl (Indiana School of Medicine) (18a) of his personal collection of sequences revealed that the carboxyl-terminal region of SSD1 is similar (29% identity over a 221-amino-acid region) to the *S. pombe* dis3 protein (Fig. 2B) (41). Cold-sensitive mutations in *dis3* cause a mitotic arrest at the nonpermissive temperature (26). It is noteworthy that *dis3* was identified in the same genetic screen and gives an arrest similar to that of *dis2*, which encodes a type 1 PPase (27). M. Goebl's computer search also revealed that the *SSD1* gene has been independently isolated from *S. cerevisiae* by R. Wilson and K. Tatchell as a suppressor (*SRK1*) of the heat shock sensitivity of a *pde2* (cyclic AMP [cAMP] phosphodiesterase) mutation and by A. Brenner, T. White, and M. Engler as a suppressor of the *ins1* mutation which results in a block in the G_1 to S transition (38). These investigators isolated *SRK1* from the same genomic library we used to isolate *SSD1*.

As assayed by the ability to suppress defects in the SIT4

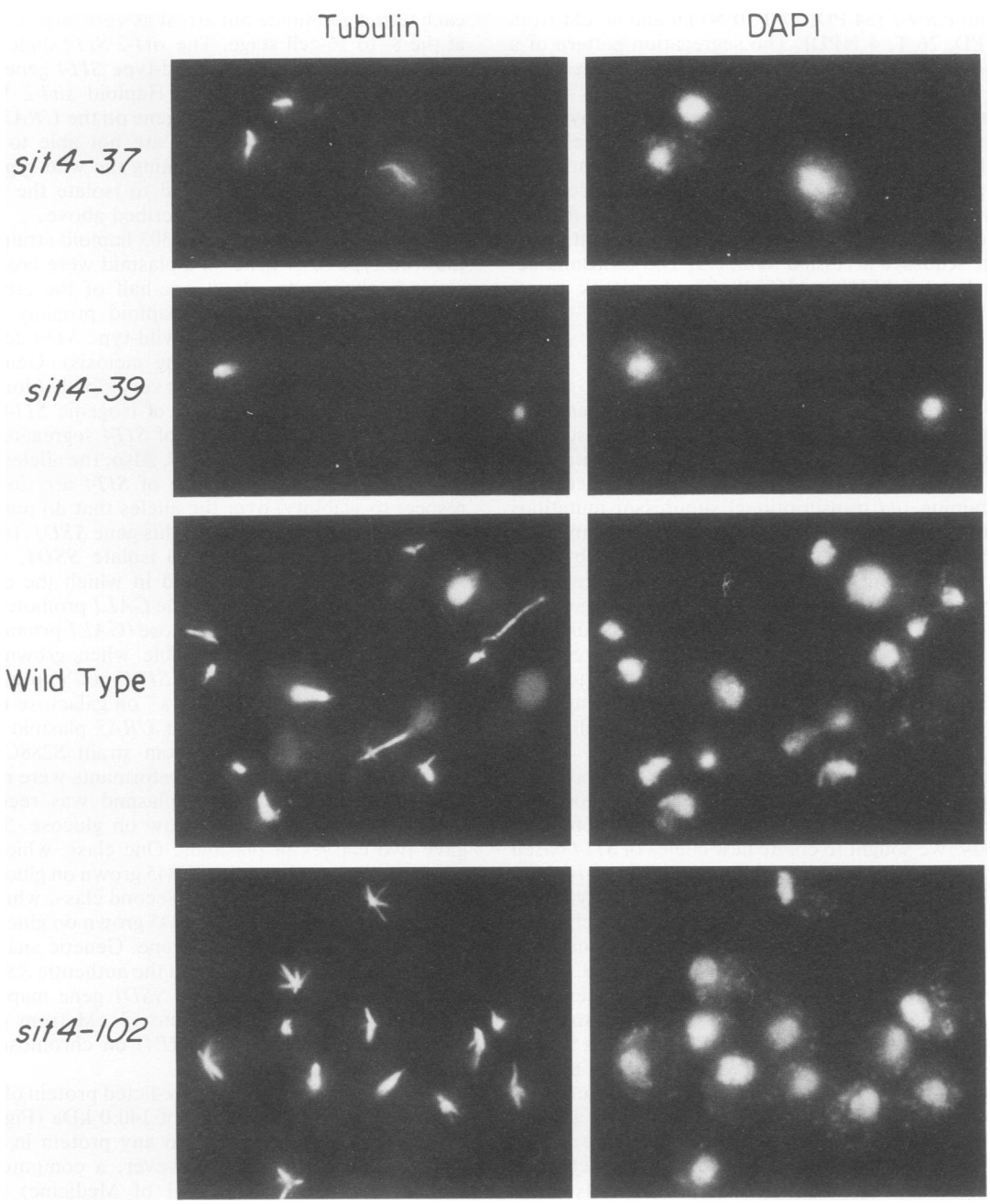

FIG. 1. G_1 arrest of *sit4* mutants. Immunofluorescence staining of tubulin and DAPI staining of DNA in strains S/A225-26-3 (*sit4-37*), S/A225-29-3 (*sit4-39*), CY49 (Wild Type), and CY93 (*sit4-102*) were done as described in Materials and Methods after incubation of strains at the nonpermissive temperature for 4.5 h. CY49 and CY93 are isogenic except for *SIT4*. An isogenic wild-type control for *sit4-37* and *sit4-39* strains gives a pattern of staining indistinguishable from that of the CY49 wild type.

phosphatase, several laboratory strains have different versions of *SSD1*. In strain YP6D, as in strain W303, deletion of *SIT4* is lethal. However, germinating YP6D haploid spores containing the *sit4-2* deletion arrest at the 1- or 2-cell stage rather than at the 8- to 16-cell stage. Genetic analysis shows that this variation is linked to *SSD1*. The version of *SSD1* in strain YP6D is called *ssd1-d1* (d for deletion of *SIT4* dead), and the version of *SSD1* in strain W303 is called *ssd1-d2*. Phenotypic variations due to *SSD1* also exist in strains where deletion of *SIT4* is viable. Deletion of *SIT4* in S288C backgrounds (*SSD1-v1* allele, v for deletion of *SIT4* viable) results in slightly lower growth rates than deletion of *SIT4* in strain L3110 (*SSD1-v2* allele). The use of capital letters for *SSD1-v* alleles is used only to indicate that these alleles are dominant to *ssd1-d* alleles with respect to viability in the absence of *SIT4*. It is important not to view *ssd1-d* alleles as mutated versions of *SSD1*. The difference between *SSD1-v* alleles and *ssd1-d* alleles is not known. Northern analysis indicates that the *SSD1* mRNA is the same length for all four *SSD1* alleles (data not shown). Also, the steady-state *SSD1* mRNA levels resulting from these four alleles are very similar, except for that of strain W303 (*ssd1-d2*), for which

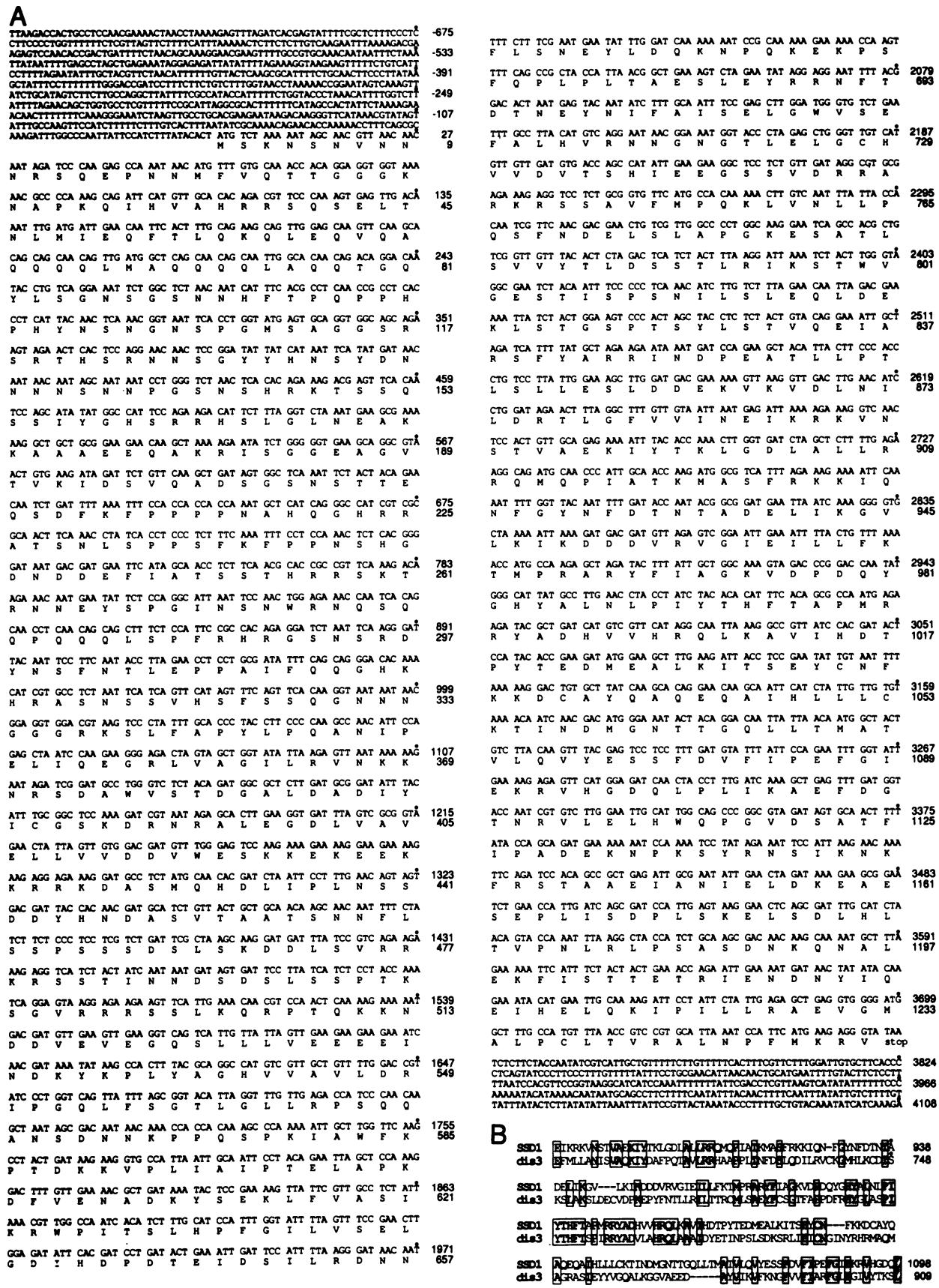

FIG. 2. *SSD1* has similarity to *dis3* of *S. pombe*. (A) The nucleotide and predicted amino acid sequence of *SSD1-v1* (accession no. M60318). (B) The SSD1 protein has a 221-amino-acid region that is similar (29% identity) to the *dis3* gene product of *S. pombe* (41). Identical amino acids are boxed. A lower degree of similarity (19% identity) between SSD1 and dis3 exists over a 307-amino-acid region on the amino-terminal side of the region shown.

the mRNA levels are about one-half the levels of the other three strains (data not shown).

Deletion of *SIT4* in strains containing *ssd1-d* alleles or in strains containing a deletion of *SSD1* (Δ*ssd1*) is lethal. Moreover, the *sit4-102* mutation results in a temperature-sensitive phenotype in *ssd1-d* or Δ*ssd1* strains. In contrast, *SSD1-v* strains containing *sit4-102* are Ts^+. Strain L3110, the background in which the original *sit4* transcriptional suppressor mutations were isolated (4), has a *SSD1-v* allele. Interestingly, in the L3110 background, the transcriptional suppressor *sit4* mutations cause a growth defect and a temperature-sensitive phenotype (Fig. 1). Moreover, strain L3110 containing a deletion of *SIT4* grows faster (and is Ts^+) than when it contains *sit4* transcriptional suppressor alleles. These results indicate that the altered SIT4 proteins encoded by the original *sit4* transcriptional suppressor alleles interfere with some function provided by the SSD1-v protein (that is not provided by the *ssd1-d* protein) and may be similar to the interfering altered dis2 protein encoded by the *dis2-11* cold-sensitive mutation (27).

***SSD1* is implicated in G_1 control.** Strains containing a deletion of *SSD1* have no readily detectable phenotypic alterations: the strains are viable, have a normal growth rate, mate normally, accumulate normal levels of glycogen upon nutrient limitation, are not temperature sensitive, and are not sensitive to nutrient limitation. In addition, flow cytometry shows that strains containing a deletion of *SSD1* have the same ratio of 1*n* to 2*n* cells as isogenic *SSD1* strains (exponential cultures in YPD medium). One phenotypic alteration of a strain containing a deletion of the *SSD1* gene is that the cell population has a smaller average cell volume (32 fl in synthetic complete medium containing 2% glucose) than isogenic *ssd1-d2* or *SSD1-v1* strains (37 fl in the same medium for both strains). This reduction in cell volume due to a deletion of *SSD1* is less than that for the *WHI1-1* (=*CLN3*) mutation (25). In addition, isogenic strains containing different *SSD1* alleles have different sensitivities to caffeine in the growth medium: strains containing a deletion of *SSD1* are the most sensitive to caffeine and *ssd1-d2* strains are moderately sensitive to caffeine, while *SSD1-v1* strains are the most resistant to caffeine (assayed at 5 to 15 mM caffeine in YPD plates). Both cell size and sensitivity to caffeine indicate that *ssd1-d2* alleles are not simply null alleles of *SSD1*. In contrast to strains containing either a deletion of *SSD1*, *ssd1-d* alleles, or *SSD1-v* alleles (in low copy number), strains containing the *SSD1-v1* gene on a high-copy-number plasmid grow more slowly than isogenic control strains and also accumulate less glycogen upon nutrient limitation.

The phenotypic defects (such as heat shock sensitivity, lack of growth on gluconeogenic carbon sources, sensitivity to nutrient limitation, and temperature sensitivity) due to disruption of the *BCY1* gene, which encodes the regulatory subunit of the cAMP-dependent protein kinases, are similar in *ssd1-d* strains as compared to strains containing a deletion of *SSD1* (data not shown). Interestingly, the *SSD1-v1* allele, in either low or high copy number, can partially suppress all of the defects due to a *BCY1* disruption in a *ssd1-d2* genetic background (Fig. 3A). Because the partial suppression of the *bcy1*::*LEU2* defects of a *ssd1-d2* strain by high-copy-number *SSD1-v1* is no better than the suppression by low-copy-number *SSD1-v1*, the difference between *ssd1-d* alleles and *SSD1-v* alleles is probably qualitative rather than quantitative. It is noteworthy that the *SSD1-v1* allele of *SSD1* which allows a strain containing a deletion of *SIT4* to be viable (but

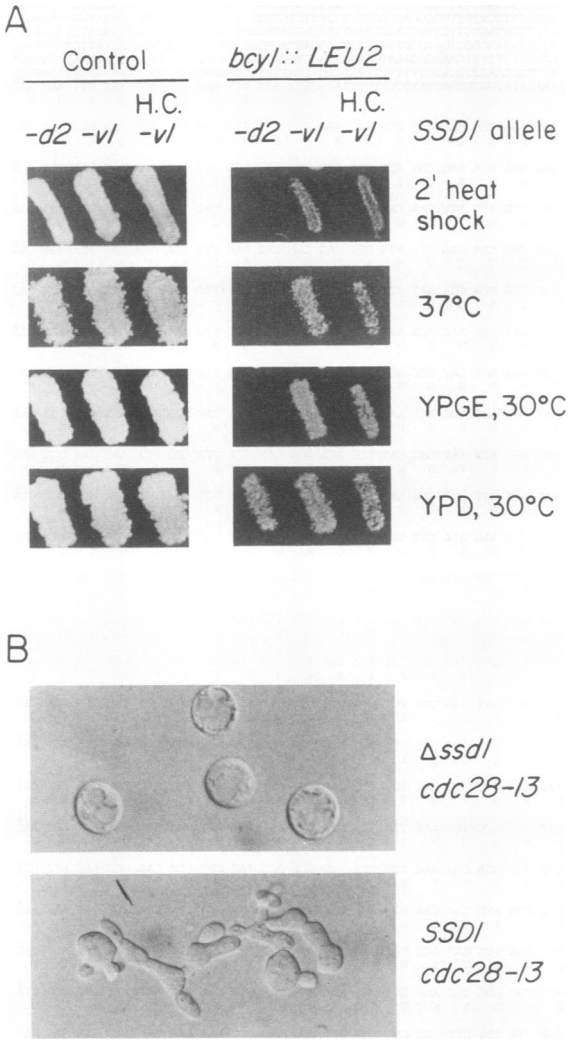

FIG. 3. Interaction of *SSD1* with *BCY1* and *CDC28*. (A) Suppression of *bcy1* defects by single-copy-number and high-copy-number *SSD1-v1*. Isogenic strains CY823 (*ssd1-d2* [*-d2*]), CY825 (*SSD1-v1* [*-v1*]), and CY827 (high-copy *SSD1-v1* [H. C. *-v1*]) were transformed to Leu^+ by using either a *LEU2*/cen plasmid (Control) or a *Bam*HI DNA fragment containing the *BCY1* gene disrupted with *LEU2* (36). Transformants were patched onto SC-Leu-Ura plates and grown at 30°C for 2 days. For the heat shock assay, the patches were replica plated onto plates prewarmed at 55°C, incubated at 55°C for 2 min, and then grown at 30°C for 2 days. Patches of the same strains were replica plated to SC-Leu-Ura plates and incubated for 2 days at 37°C or replica plated onto YPGE and YPD and incubated for 2 days at 30°C. (B) A deletion of *SSD1* alters the arrest morphology of *cdc28-13*. Strain CY81 (*cdc28-13*) was crossed to strain CY798 (*ssd1*::*LEU2*) and sporulated, and tetrads were dissected. In all 18 of the tetrads examined, strains containing the double *ssd1*::*LEU2 cdc28-13* mutations arrested (37°C, overnight) as large round cells as shown in the upper panel, while strains with the single *cdc28-13* mutation arrested (37°C, overnight) with the shmoo morphology shown in the lower panel. After only 4 h at 37°C, each *ssd1*::*LEU2 cdc28-13* culture was composed of about one-third slightly shmoo-shaped cells and two-thirds round cells. At this time (4 h at 37°C), both populations of *ssd1*::*LEU2 cdc28-13* cells were larger than *cdc28-13* cells. As the time at 37°C increased, the population of *ssd1*::*LEU2 cdc28-13* cells that had a slight shmoo shape gradually became round and both populations of *ssd1*::*LEU2 cdc28-13* cells grew larger. After 12 h at 37°C, the cells appeared as shown.

to grow very slowly) is the form of *SSD1* that can partially suppress all of the defects due to a *BCY1* disruption.

Mutations in *SSD1* also interact with the CDC28 pathway. Normally, *cdc28-13* strains arrest at the nonpermissive temperature in a G_1-like state with elongated projections (possibly representing aberrant bud formation). In contrast, *cdc28-13* strains containing a deletion of *SSD1* arrest at the nonpermissive temperature with a completely different morphology: the cells become large, appear swollen, and become round with no projection (Fig. 3B).

SIT4 functions in late G_1 for progression into S phase. To more precisely map the G_1 arrest point due to temperature-sensitive mutations in *SIT4*, the following experiments were performed. Strain CY738 (*MATa sit4-102 ssd1-d1*) was arrested at the nonpermissive temperature for 4.5 h and then simultaneously shifted to the permissive temperature and treated with α factor. These cells did not form buds or undergo cell division but began to take on the characteristic morphology of α-factor-arrested cells. Similar results were obtained with a *MAT***a** *cdc28-13* strain. Therefore, strains containing temperature-sensitive mutations in either *sit4* or *cdc28* arrest in G_1 at a point that is sensitive to α factor. In addition, both *sit4-102* strains and *cdc28-13* strains arrested at the nonpermissive temperature are able to mate (data not shown). This G_1 arrest of *sit4* haploid strains at the nonpermissive temperature is not due to inappropriate induction of the mating pathway because homozygous *sit4/sit4* diploids also have a temperature-sensitive phenotype.

To define the SIT4 execution point, strain CY738 (*MAT***a** *sit4-102 ssd1-d1*) was first arrested in G_1 by α factor treatment at the permissive temperature. The cells were then washed and resuspended in fresh medium. At 5-min intervals after α-factor release, aliquots of the culture were shifted to the nonpermissive temperature (37°C). When the cells were shifted to the nonpermissive temperature at any time before the cells formed a visible bud (visible bud formation occurs very near initiation of S phase), the cells did not enter the cell cycle but arrested as unbudded G_1 cells. When the cells were shifted to the nonpermissive temperature at any time after the cells formed a visible bud, the cells continued through the cell cycle and then arrested in G_1. When this type of experiment was repeated with a *MAT***a** *cdc28-13* strain (MDMy256), the results were identical to those with the *sit4-102* strain. In contrast, *MAT***a** *cdc25-1* cells (strain T25-1) that were released from α-factor arrest were not sensitive to arrest in G_1 at the nonpermissive temperature until they entered and completed the cell cycle. Strains containing temperature-sensitive mutations in *CDC25* (whose product is required for activation of the cAMP-dependent protein kinases [15]) arrest in a state similar to the nutritional arrest point. Therefore, in contrast to CDC25, both SIT4 and CDC28 are required in late G_1 for progression into S phase.

***sit4* strains have phenotypes associated with defects in G_1 control.** Strains containing *sit4* transcriptional suppressor alleles are unable to utilize glycerol or ethanol as carbon sources (4). In addition, these strains are unable to grow on acetate. The inability to utilize nonfermentable carbon sources is characteristic of mutants altered in the cAMP-dependent protein kinase pathway. Furthermore, like strains containing mutations that reduce the activation of the cAMP-dependent protein kinases, strains containing transcriptional suppressor *sit4* mutations hyperaccumulate glycogen compared with wild-type strains (Fig. 4A). Because one of the effects of caffeine is to inhibit cAMP phosphodiesterases (6), we determined the effect of caffeine on the growth of *sit4* strains. In striking contrast to the growth of an isogenic wild-type strain, the growth of strains containing transcriptional suppressor *sit4* mutations is actually stimulated by the presence of caffeine in the growth medium (Fig. 4B).

To look for gene interactions between *SIT4* and other genes whose products act in G_1, we disrupted the *BCY1* gene in a *sit4-102* (*ssd1-d2*) strain and an isogenic *SIT4* (*ssd1-d2*) strain by transformation. Colonies of all four types of isogenic transformants appeared on the transformation plates at about the same time and were of similar size. However, when these transformants were streaked for single colonies at the permissive temperature 2 days after the transformation, very few of the *sit4-102 bcy1-2* (*ssd1-d2*) cells were viable (Fig. 4C). Although inviability upon nutrient limitation is a phenotype of *bcy1* mutants (in which 5- to 6-day-old colonies become inviable), the inviability of *sit4-102 bcy1-2* (*ssd1-d2*) double mutants is seen in 1.5-day-old transformants. Since the *sit4-102 bcy1-2* (*ssd1-d2*) transformant cells initially give rise to single colonies, it is possible that the delayed lethality is due to dilution of the BCY1 protein as the cells divide. The specificity of this synthetic lethality is demonstrated by the fact that *sit4-102 bcy1-2* double mutants are viable in a *SSD1-v* background.

We also looked for gene interactions between *sit4* and *cdc28* mutations. At permissive temperatures, the transcriptional suppressor mutations *sit4-36* or *sit4-258* are lethal in combination with the *cdc28-13* mutation (data not shown). More dramatically, *sit4-102* in combination with *cdc28-13* results in extremely large cells at 30°C (Fig. 4D). In contrast, strains containing either *sit4-102* or *cdc28-13* alone grow almost normally at this temperature.

The SIT4 protein is localized to the cytoplasm. To determine the localization of the SIT4 protein, antibodies were raised against a peptide corresponding to amino acid residues 1 to 16 of the SIT4 protein. The amino-terminal region of SIT4 was chosen because this region is not conserved between type 1, type 2A, and SIT4 PPases. The affinity-purified antibodies recognize only SIT4 in Western analysis of extracts prepared from yeast (Fig. 5B). These antibodies were used for indirect immunofluorescence staining of asynchronous yeast cells containing the *SIT4* gene on a high-copy-number 2μm vector (Fig. 5A). These data show that the majority of the SIT4 protein is localized to the cytoplasm and excluded from the nucleus. We cannot detect any obvious differences in the SIT4 localization in cells at different stages of the cell cycle. Similar results were obtained from strains in which *SIT4* is present in single copy number, although the staining is faint (data not shown). A *SSD1-v* strain containing a deletion of the *SIT4* gene shows almost no background staining (Fig. 5A).

To rule out the possibility that the nuclear exclusion of SIT4 observed in the immunofluorescence analysis resulted from an inability of the antibodies to enter the nucleus, extracts of wild-type yeast cells were fractionated into crude nuclear (P25) and cytoplasmic (S25) fractions (see Materials and Methods). Western analysis of these fractions shows that SIT4 is found exclusively in the cytoplasmic fraction (Fig. 5C). The same localization is seen for CDC28, as was previously reported (40). In contrast, the SIS1 protein, which by indirect immunofluorescence is localized to both the nucleus and cytoplasm (32a), is found in both the nuclear and cytoplasmic fractions.

The SIT4 phosphatase associates with two high-molecular-weight phosphoproteins. While the antibodies directed against the SIT4 amino-terminal peptide are suitable for

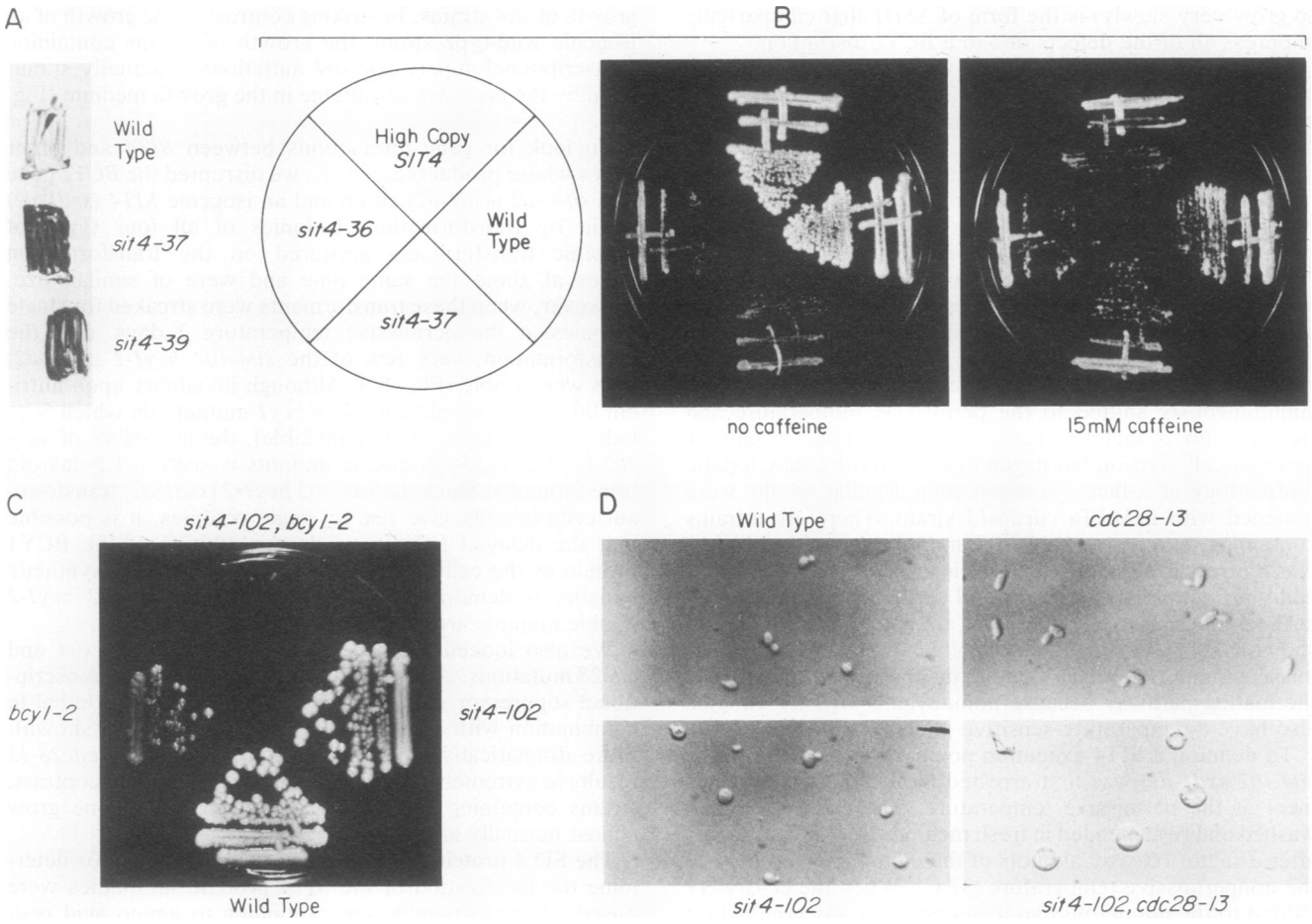

FIG. 4. Phenotypes of *sit4* strains. (A) Glycogen accumulation. Patches of the isogenic strains L3110 (Wild Type), S/A225-26-3 (*sit4-37*), and S/A225-29-3 (*sit4-39*) were grown for 2 days on SC-Ura plates and then inverted over iodine crystals for 5 min. (B) Caffeine stimulates the growth of *sit4* strains. Isogenic strains AY953 (High Copy *SIT4*), AY910 (Wild Type), S/A225-26-3 (*sit4-37*), and S/A225-23-5 (*sit4-36*) were grown for 2 days at 30°C on GNA plates containing no caffeine or 15 mM caffeine. (C) Synthetic lethality of *sit4-102 bcy1-2* double mutants. Isogenic strains CY93 (*sit4-102 ura3-1*) and CY105 (*SIT4 ura3-1*) were transformed to Ura^+ with a *Bam*HI fragment containing the *BCY1* gene disrupted with *URA3* to create *bcy1-2 sit4-102* or *bcy1-2 SIT4* strains. For controls, wild-type and *sit4-102* strains were transformed with *Nco*I-cut YIp5 to direct integration of the *URA3* gene to the chromosome. Two days after the transformation, Ura^+ colonies were restreaked onto SC-Ura plates and grown for 2 days at 30°C. (D) Interaction with *CDC28*. Strain CY240 (*cdc28-13*) was crossed to CY146 (*sit4-102*) and sporulated, and tetrads were dissected. Progeny from one tetratype which produced the indicated combinations of alleles were grown overnight at 24°C in YPD and then shifted to 30°C (a permissive temperature for *sit4-102* and a semipermissive temperature for *cdc28-13*) for 4 h. Three different tetratype tetrads gave similar results. The extremely-large-cell phenotype at 30°C was observed for all *sit4-104 cdc28-13* double mutants. Pictures were taken with a Nikon optiphot microscope with Nomarski optics.

indirect immunofluorescence and Western analysis, they do not efficiently immunoprecipitate native SIT4 from yeast extracts. For immunoprecipitation analysis, the SIT4 protein was tagged with a 9-amino-acid epitope for which a high-affinity monoclonal antibody is available (12CA5 [17]). The 12CA5 monoclonal antibody has low cross-reactivity to endogenous yeast proteins. To epitope tag the SIT4 protein, a DNA sequence encoding a 9-amino-acid influenza hemagglutinin antigen was inserted into the *SIT4* gene at a position corresponding to either the extreme amino terminus or the extreme carboxyl terminus of the SIT4 protein (see Materials and Methods). An isogenic set of three W303 *ssd1-d2* strains was prepared which differed only in the source of SIT4 protein: one strain contained only wild-type SIT4 without the epitope tag, one strain contained only amino-terminally tagged SIT4, and another strain contained only carboxyl-terminally tagged SIT4. The epitope tagged SIT4 proteins are functional since the strains containing only the tagged forms of SIT4 have nearly the same growth rate (doubling times of 95 min for amino-terminally tagged SIT4 and 84 min for carboxyl-terminally tagged SIT4, in YPD) as an isogenic strain containing wild-type SIT4 (doubling time = 70 min, in YPD). The absence of SIT4 in strain W303 (*ssd1-d2*) is lethal.

The epitope-tagged SIT4 protein can be efficiently immunoprecipitated from extracts prepared from ^{35}S-labeled yeast cells (Fig. 6). The SIT4 protein migrates at slightly different positions depending on whether the epitope is at the amino terminus or at the carboxyl terminus of the protein. Two proteins, with apparent molecular masses of 155 and 190 kDa, specifically coimmunoprecipitate with SIT4 (Fig. 6). Immunoprecipitation of extracts prepared from cells labeled

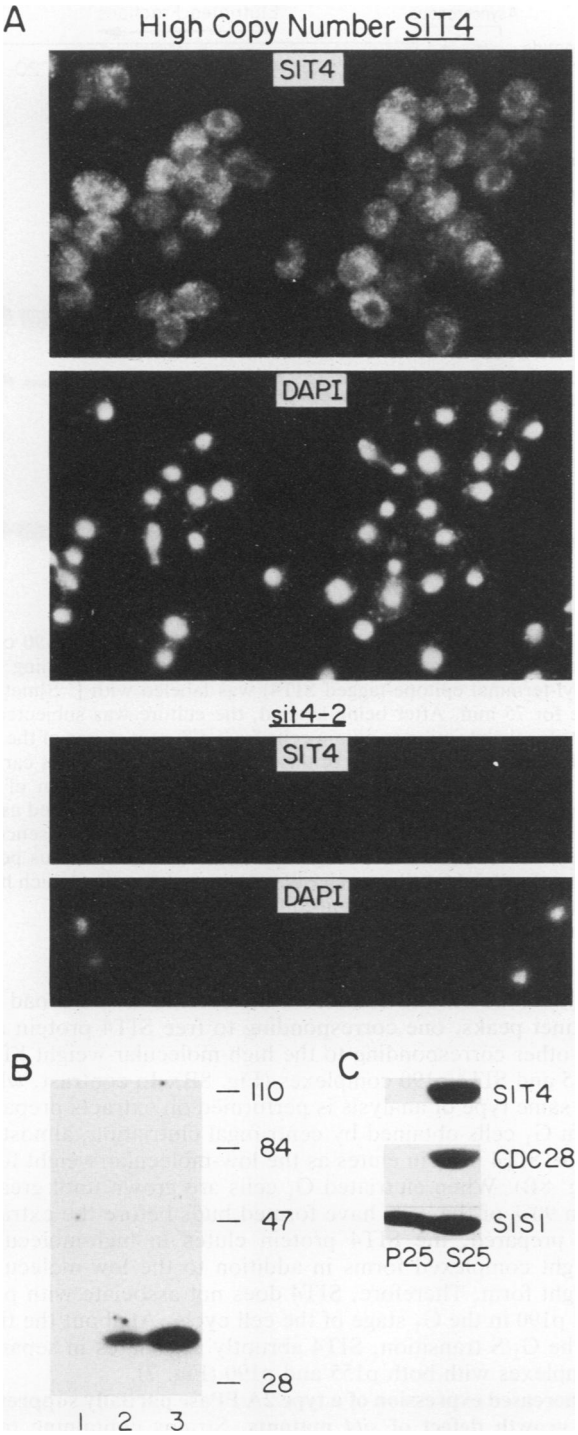

FIG. 5. SIT4 is localized to the cytoplasm. (A) Immunofluorescence microscopy. Indirect immunofluorescence using affinity-purified anti-SIT4 peptide antibodies and DAPI staining of asynchronous cells was done as described in Materials and Methods. The high-copy-number *SIT4* results were obtained by using strain CY198 in which the *SIT4* gene is on a high-copy-number 2μm vector. The *sit4-2* results were obtained by using strain CY248 (*sit4-2 SSD1-v1*), in which almost the entire *SIT4* coding region has been deleted. (B) Specificity of the anti-SIT4 antibody. The specificity of the anti-SIT4 peptide antibodies used in these studies was determined by Western immunoblotting. Extracts prepared from the indicated strains were subjected to sodium dodecyl sulfate–10% polyacrylamide gel electrophoresis before immunoblotting. Lane 1, CY248 (*sit4-2* deletion); lane 2, CY199 (*sit4-2* plus *SIT4* on a low-copy-number vector); lane 3, CY198 (*sit4-2* plus *SIT4* on a high-copy-number vector). Molecular masses (in kilodaltons) of standards are indicated on the right. (C) Subcellular fractionation. An extract prepared from an exponentially growing culture of CY199 (containing wild-type *SIT4* on a low-copy-number plasmid) was fractionated into a crude nuclear pellet (P25) and postnuclear cytoplasmic fraction (S25). Protein from equal numbers of cells was subjected to sodium dodecyl sulfate-polyacrylamide gel electrophoresis followed by Western analysis. For the cytoplasmic fraction, 0.38 mg of protein was added to each lane. For the nuclear fraction, 0.074 mg protein was added to each lane. The antibodies used were anti-SIT4 peptide antibody, an antibody directed against a synthetic peptide corresponding to the amino terminus of CDC28 (donated by B. Futcher), and antibody directed against a trpE-SIS1 fusion protein.

with $^{32}P_i$ shows that both p155 and p190 are phosphorylated in vivo (Fig. 6). In contrast, SIT4 is not detectably phosphorylated in vivo.

Neither p155 nor p190 are encoded by *SSD1*. Immunoprecipitations of *SIT4* from isogenic strains containing a deletion of *SSD1*, the *ssd1-d2* allele, the *SSD1-v1* allele, or the *SSD1-v1* allele on a high-copy-number vector yield immunoprecipitation patterns identical to those shown in Fig. 6. Therefore, *SSD1* can not encode p155 or p190. We can not exclude the possibility that *SSD1* encodes a protein that associates with SIT4 but is not detected in our immunoprecipitation assays.

The association of SIT4 with p155 and p190 is cell cycle regulated. Western analysis of extracts prepared from cells synchronized by either α factor or centrifugal elutriation shows that the steady-state levels of SIT4 do not vary in the cell cycle (data not shown). In contrast, the association of SIT4 with p155 and p190 is regulated in the cell cycle. In order to obtain uniformly labeled cells from different stages of the cell cycle, an asynchronous culture of strain CY202 containing the carboxyl-terminally tagged SIT4 protein was grown in the presence of [^{35}S]methionine for 75 min and then subjected to centrifugal elutriation. Extracts were prepared from fractions containing cells at different stages of the cell cycle. Immunoprecipitation of SIT4 from extracts prepared from cells in the later stages of the cell cycle contain both p155 and p190 (Fig. 7). In contrast, p155 and p190 are not detectable when SIT4 is immunoprecipitated from extracts prepared from G_1 cells (Fig. 7). Similar results were obtained by immunoprecipitation of epitope-tagged SIT4 from extracts prepared from synchronous (synchronized by either α factor or centrifugal elutriation) populations of cells that were labeled for 20 min at different stages of the cell cycle (data not shown).

The possibility exists that the cell-cycle-dependent association of SIT4 with p155 and p190 does not occur with wild-type SIT4 but is specific only to SIT4 that has been epitope tagged. Also, one could argue that the lack of observable p155 and p190 in SIT4 immunoprecipitates from extracts prepared from G_1 cells is due to ^{35}S-labeling artifacts. To rule out these possibilities, gel filtration chromatography was used to separate SIT4 into high- and low-molecular-weight forms. To test the validity of this approach, an extract prepared from an asynchronous ^{35}S-labeled culture of a strain containing epitope-tagged SIT4 was fractionated on a Sephadex G200 column. Immunoprecipitation of these column fractions shows that about half of the epitope-tagged SIT4 elutes as a low-molecular-mass form at about 40 kDa, probably corresponding to free monomeric

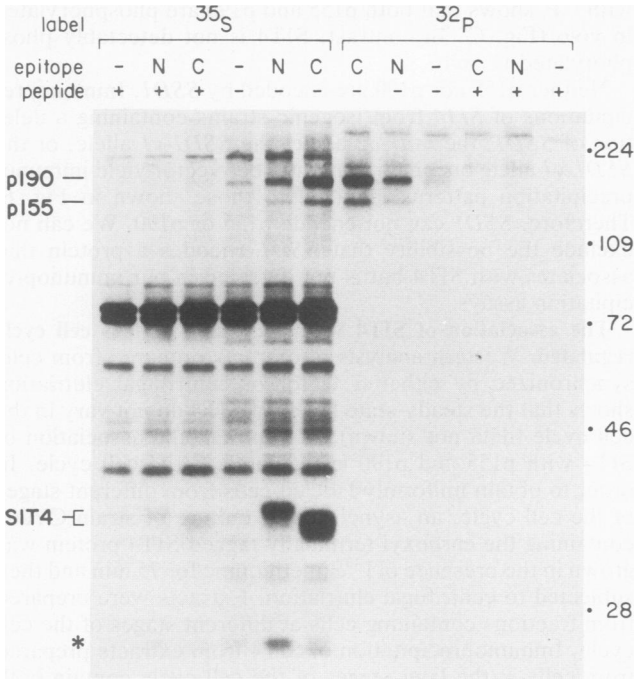

FIG. 6. Coimmunoprecipitation of p155 and p190 with SIT4. These experiments used three isogenic strains: strain CY200, which contains the SIT4 protein epitope tagged at the amino terminus (N); CY202, which contains the SIT4 protein epitope tagged at the carboxyl terminus (C); and CY199, which contains wild-type SIT4 (−). The cells were labeled with [^{35}S]methionine or $^{32}P_i$. Extracts were prepared and immunoprecipitated by using 0.5 μl of MAb 12CA5 ascites directed against the epitope. The immunoprecipitates were subjected to sodium dodecyl sulfate-polyacrylamide gel electrophoresis in an 8% gel, followed by autoradiography. Where indicated (+), the antibody was incubated with 10 μg of the competing HA peptide for 30 min prior to addition to extracts. p155 and p190 refer to proteins which specifically coimmunoprecipitate with SIT4. A band that migrates just below p190 precipitates with the 12CA5 antibody but is not specific to epitope-tagged SIT4. p190 is the upper band in the doublet at 190 kDa in the ^{35}S-labeled N and C lanes. The SIT4 protein migrates slightly differently depending upon whether the epitope is at the amino or carboxyl terminus. The asterisk marks the position, in the fifth and sixth lanes, of SIT4 degradation products that we routinely see in our extracts. These bands were identified as SIT4 degradation products by Western analysis. The increased intensity in the fifth and sixth lanes at about 48 kDa has not been consistently observed in our numerous immunoprecipitation experiments.

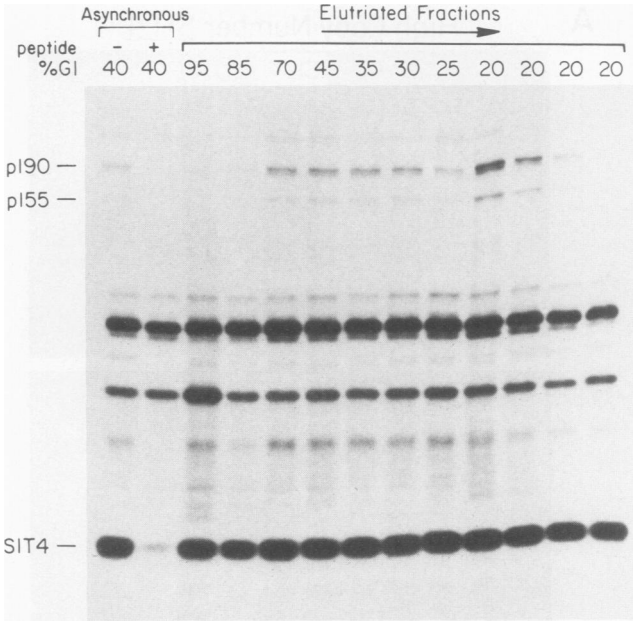

FIG. 7. Cell cycle regulation of SIT4/p155 and SIT4/p190 complexes. An asynchronous culture of strain CY202 (containing carboxyl-terminal epitope-tagged SIT4) was labeled with [^{35}S]methionine for 75 min. After being labeled, the culture was subjected to centrifugal elutriation to obtain cells from different stages of the cell cycle. Immunoprecipitation of the epitope-tagged SIT4 was carried out on extracts prepared from these fractions. A portion of the labeled cells were removed prior to elutriation and processed as for Fig. 6 to show the immunoprecipitation pattern (in the presence or absence of 10 μg of competing peptide) of an asynchronous population of cells. %G1, Percentage of cells in each fraction which have a 1*n* DNA content as determined by flow cytometry.

SIT4 (Fig. 8A). The other half of the epitope-tagged SIT4 protein elutes in high-molecular-weight complexes with p155 and p190 (Fig. 8A). The p190/SIT4 complex elutes at a slightly higher molecular weight than the p155/SIT4 complex, demonstrating that SIT4 is in separate complexes with p155 and p190.

The above results show that the association of SIT4 with p155 and p190 can be determined by looking directly at the partitioning of SIT4 between a low-molecular-weight form and high-molecular-weight complexed forms. This type of analysis eliminates ^{35}S-labeling artifacts. Extracts prepared from asynchronous cells containing wild-type SIT4 protein were fractionated on a Sephadex G200 column. The levels of wild-type SIT4 protein in each fraction were determined by Western analysis using the antibody directed against the SIT4 amino-terminal peptide. For this analysis, wild-type SIT4 can be seen to elute from the column in two broad but distinct peaks, one corresponding to free SIT4 protein and the other corresponding to the high-molecular-weight SIT4/p155 and SIT4/p190 complexes (Fig. 8B). In contrast, when the same type of analysis is performed on extracts prepared from G_1 cells obtained by centrifugal elutriation, almost all of the SIT4 protein elutes as the low-molecular-weight form (Fig. 8B). When elutriated G_1 cells are grown until greater than 90% of the cells have formed buds before the extracts are prepared, the SIT4 protein elutes in high-molecular-weight complexed forms in addition to the low-molecular-weight form. Therefore, SIT4 does not associate with p155 and p190 in the G_1 stage of the cell cycle. At about the time of the G_1/S transition, SIT4 abruptly associates in separate complexes with both p155 and p190 (Fig. 7).

Increased expression of a type 2A PPase partially suppresses the growth defect of *sit4* mutants. Strains containing transcriptional suppressor *sit4* mutations (4) grow very slowly, having doubling times of about 300 min in YPD at 30°C (compared with 109 min for isogenic *SIT4* strain L3110, in YPD). To identify substrates of SIT4, proteins that regulate SIT4, or proteins that can functionally substitute for SIT4, we searched for wild-type genes that in high copy number can suppress the growth defect of *sit4* strains. This screen yielded four different wild-type genes that in high copy number can partially suppress the growth defect due to three different *sit4* transcriptional suppressor mutations. These genes in high copy number do not increase the growth rate of wild-type strains, do not reduce the original His$^+$ suppres-

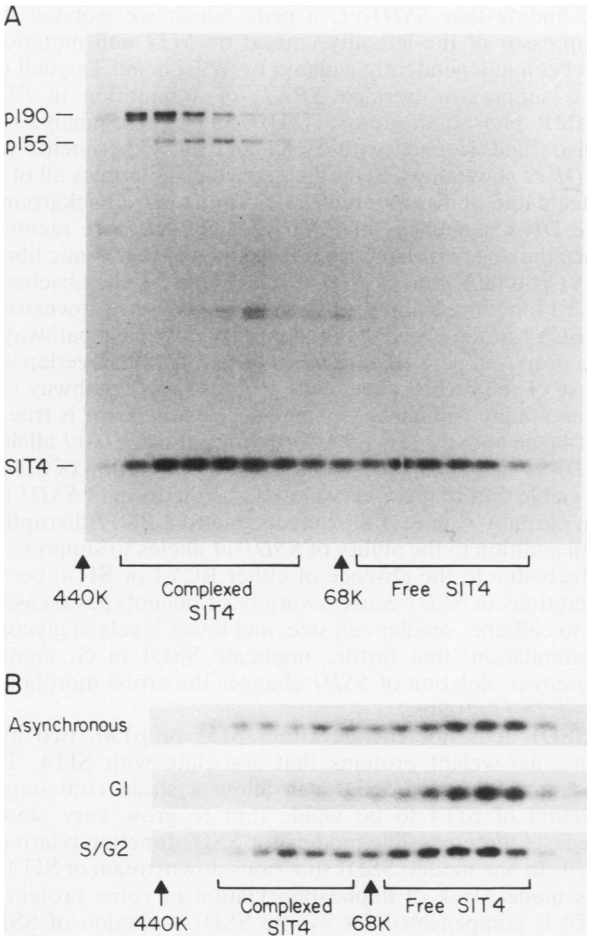

FIG. 8. Separation of SIT4 complexes by gel filtration chromatography. (A) Gel filtration and immunoprecipitation of labeled cell extracts. Strain CY202 (containing carboxyl-terminal epitope-tagged SIT4) was labeled with [^{35}S]methionine for 75 min. Then, 0.6 ml of an extract prepared from the labeled cells was applied to a Sephadex G200 column (1.5 by 28.3 cm) and 0.8-ml fractions were collected. Proteins from every other fraction were immunoprecipitated with MAb 12CA5 ascites (0.5 μl) and subjected to sodium dodecyl sulfate-polyacrylamide gel electrophoresis and autoradiography. Molecular mass markers 440K and 68K correspond to the peaks of ferridoxin and bovine serum albumin, respectively, run on the same column. (B) Gel filtration and Western analysis of wild-type SIT4. Extracts from either asynchronous, G_1, or S/G_2 populations of strain CY199 (containing wild-type SIT4) were prepared as described in Materials and Methods. These extracts were fractionated on a Sephadex G200 column (1.5 by 26.3 cm), and 0.8-ml fractions were collected. Proteins from every other fraction were precipitated by TCA and subjected to sodium dodecyl sulfate-polyacrylamide gel electrophoresis and Western analysis. The antibody used as probe for SIT4 was the anti-SIT4 peptide antibody. Before TCA precipitation, a small amount of a control protein was added to each fraction. Subsequent Western analysis of the same blot showed that the levels of the control protein varied by less than 10% between lanes. Molecular mass markers 440K and 68K correspond to the peaks of ferridoxin and bovine serum albumin, respectively, run on the same column.

sion phenotype resulting from the *sit4* mutations (4), and do not suppress the temperature sensitivity of any *sit4* strains.

One of these four genes, termed *PPH2α*, encodes a predicted protein of 377 amino acids (43.0 kDa) that is 80% identical to the catalytic domain of mammalian type 2A PPases (Fig. 9). This similarity extends to the extreme carboxyl terminus. PPH2α is predicted to have an acidic (net charge of −17) amino-terminal region not present in other type 1, type 2A, or SIT4 PPases. This unique amino-terminal region is probably encoded because greater than 90% of *PPH2α* mRNA initiates upstream of the first ATG codon of this amino-terminal region (Fig. 9). The function of this acidic amino-terminal extension is not known. The *PPH2α* gene maps to a previously unidentified genetic locus, 16.7 cM from *CDC9* (gene order: *PPH2α CDC9 CDC2*) on chromosome IV (see Materials and Methods). While *PPH2α* in high copy number can increase the growth rate of strains containing transcriptional suppressor *sit4* mutations, *PPH2α* in high copy number does not allow growth of a *ssd1-d* strain containing a deletion of *SIT4*. Therefore, overexpressed PPH2α can not replace the function of SIT4. Deletion of *PPH2α* either in wild-type *SIT4* strains or in *SSD1-v* strains containing a deletion of *SIT4* causes no obvious phenotypic alterations. However, *S. cerevisiae* has a second type 2A PPase, termed PPH2β (22a), that is 98% identical to the PPH2α protein over a 325-amino-acid overlap.

DISCUSSION

The SIT4 PPase functions in late G_1 for progression into S phase. At the nonpermissive temperature, strains containing temperature-sensitive *sit4* mutations arrest without a visible bud, with an unduplicated spindle pole body, and with a 1*n* DNA content. In *S. cerevisiae*, bud emergence, spindle pole body duplication, and initiation of DNA synthesis occur almost simultaneously and mark the beginning of S phase. Order-of-function mapping defines the SIT4 execution point to late G_1, at or extremely close to the execution point of CDC28. The SIT4 execution point, in addition to the increase in cell size and mating competence of *sit4* mutants arrested at the nonpermissive temperature, identifies *SIT4* as a class I start gene (28). This is in contrast to class II genes, which include *CDC25* and *CDC35*; strains containing temperature-sensitive mutations in these genes arrest at a point similar to that caused by nutritional limitation (23).

Mutations in *SIT4* interact with mutations in both *BCY1* (regulatory subunit of the cAMP-dependent protein kinases) and *CDC28*. For *CDC28*, the transcriptional suppressor *sit4* alleles are lethal in combination with *cdc28-13* and the *sit4-102* allele in combination with *cdc28-13* causes the cells to become extremely large. For *BCY1*, strains containing both *sit4-102* and *bcy1::URA3* mutations (in an *ssd1-d* background) are inviable, even though either mutation alone causes only a small to moderate growth defect. That the *sit4-102* mutation causes lethality in the absence of the BCY1 protein indicates that SIT4 probably functions downstream of BCY1 or in a possible parallel pathway whose functions overlap with the cAMP-dependent protein kinase pathway (35). In addition to these gene interactions, the transcriptional suppressor *sit4* mutations cause a variety of phenotypes (glycogen accumulation, caffeine resistance, and inability to grow on nonfermentable carbon sources) which are characteristic of certain mutations in the cAMP-dependent protein kinase pathway. Although the molecular mechanisms leading to these effects are not known, the gene interactions and the *sit4* phenotypes indicate that SIT4 may interact with both the cAMP-dependent protein kinase and CDC28 protein kinase pathways.

Additional evidence suggesting that SIT4 interacts with the cAMP-dependent protein kinase pathway comes from

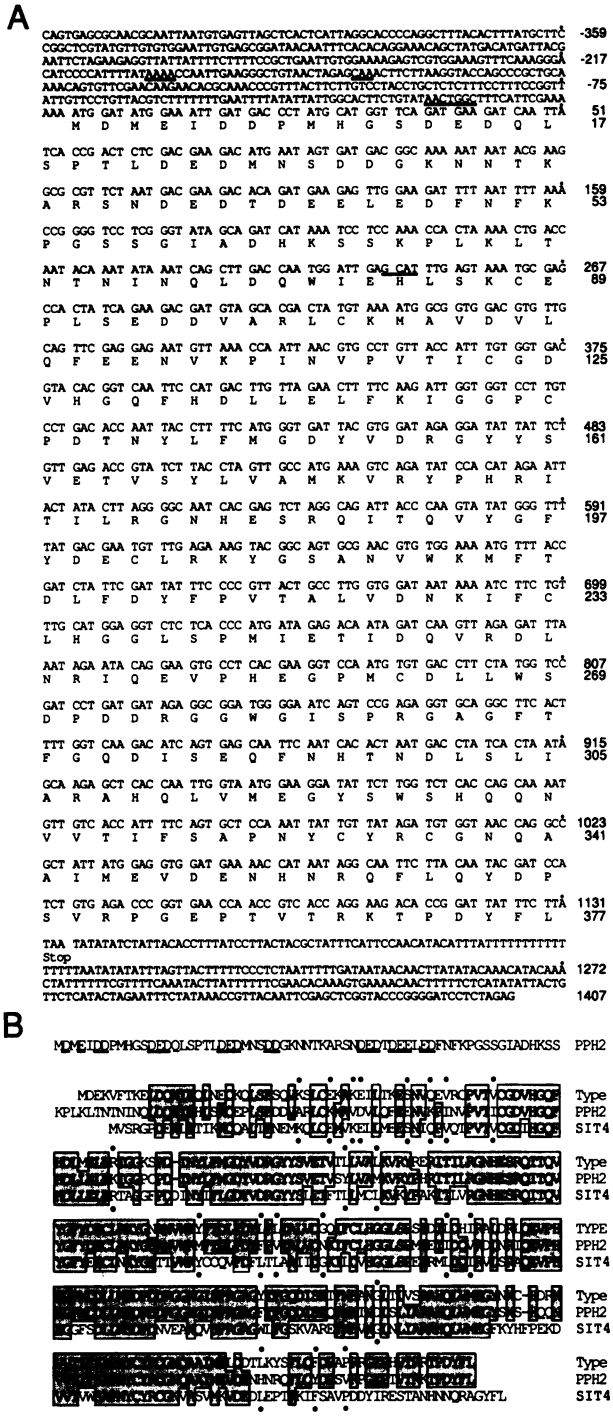

FIG. 9. *PPH2*α encodes a type 2A PPase. (A) Nucleotide sequence of *PPH2*α (accession no. M60317). The sequenced DNA fragment contains a single large open reading frame (nucleotides 1 to 1131) which encodes a predicted protein of 377 amino acids. The underlined nucleotides indicate the 5′ end of the *PPH2*α mRNA determined by primer extension analysis. Greater than 90% of the mRNA initiates upstream of the indicated *PPH2*α ATG start codon. (B) The *PPH2*α gene encodes a protein with similarity to type 2A PPases. The *PPH2*α predicted amino acid sequence is compared with the sequences of the catalytic subunit of rabbit skeletal muscle type 2A phosphatase (14) and SIT4 (4). Identical amino acid residues are boxed. The dots indicate amino acid residues that are shared between SIT4 and mammalian type 2A PPase but are not conserved in PPH2α. The first line shows the acidic amino-terminal extension which is unique to PPH2α.

the finding that *SSD1-v1*, a gene which we isolated as a suppressor of the lethality caused by *SIT4* null mutations, has been independently isolated by Wilson and Tatchell (38) as a suppressor (termed *SRK1*) of a mutation in *PDE2* (cAMP phosphodiesterase [31]). Subsequent analysis by Wilson and Tatchell with *SRK1* and our experiments with *SSD1-v1* show that *SSD1-v1* can partially suppress all of the defects due to disruption of *BCY1* (in a *ssd1-d* background). The DNA sequences of *SSD1-v1* and *SRK1* are identical, since they were isolated from the same yeast genomic library in YCp50 (30). Since *SSD1-v1* can suppress the absence of BCY1 function, SSD1 probably functions either downstream of BCY1 in the cAMP-dependent protein kinase pathway or in a proposed parallel pathway whose functions overlap with those of the cAMP-dependent protein kinase pathway (35). Interestingly, similar reasoning suggests the same is true for SIT4 (see above). It is noteworthy that the *SSD1-v1* allele of *SSD1*, which allows a strain containing a deletion of *SIT4* to be viable (but to grow very slowly), is the form of *SSD1* that can partially suppress the defects due to a *BCY1* disruption.

In addition to the ability of *SSD1-v1* alleles to suppress the defects due to the absence of either BCY1 or SIT4, certain alterations in *SSD1* cause a variety of phenotypes (sensitivity to caffeine, smaller cell size, and lower levels of glycogen accumulation) that further implicate SSD1 in G_1 control. Moreover, deletion of *SSD1* changes the arrest morphology of *cdc28-13* strains.

SSD1 does not encode either p155 or p190, two high-molecular-weight proteins that associate with SIT4. That certain versions of SSD1 can allow a strain containing a deletion of SIT4 to be viable (but to grow very slowly) suggests three possible models for SSD1 function relative to SIT4. In one model, SSD1 functions downstream of SIT4. In this model, lack of dephosphorylation of some protein by SIT4 is compensated for by the SSD1-v version of SSD1. Here, SSD1 could be a substrate of SIT4 that can partially function (in the SSD1-v version) without the normal regulation of its phosphorylation state by SIT4. In the second model, SSD1 could function as a phosphatase that, in the SSD1-v version, can partially dephosphorylate the SIT4 substrates. However, SSD1 has no similarity to known protein phosphatases. In the third model, the SSD1-v version of SSD1 can provide some function in a parallel pathway to the SIT4 pathway that is not provided by the ssd1-d version of the protein. In this model, SSD1 could function as a positive regulator of another phosphatase. Here, the SSD1-v version of SSD1 could target another phosphatase to substrates that are normally primarily dephosphorylated by SIT4. That SSD1 could interact with a protein phosphatase is suggested by the region of similarity of SSD1 to the dis3 protein of *S. pombe* (41). A mutation in *dis3* is lethal in combination with a mutation in *dis2* (41), which encodes a predicted type 1 PPase (27). If SSD1-v does target another phosphatase(s) to the SIT4 substrate, the primary PPase cannot be PPH2α. *SSD1-v1* strains containing a deletion of *SIT4* show no additional growth defect when the *PPH2*α is also deleted.

SIT4 probably defines a class of phosphatase that is distinct from type 1 and type 2A PPases. SIT4 is about 55% identical to mammalian type 2A PPases and 40% identical to mammalian type 1 PPases. This is about the same amount of similarity shared between mammalian type 1 and type 2A PPases. Also, *S. cerevisiae* contains a close homolog of mammalian type 1 PPases (27) and two close homologs of mammalian type 2A PPases (PPH2α and PPH2β). Even when PPH2α is overexpressed, it cannot cure the lethality

caused by deletion of *SIT4* in a *ssd1-d* background. Of known phosphatases, SIT4 is slightly more similar to the catalytic domains of PPX (59% identity [12]) and of PPV (62% identity [13]) than to type 2 PPases (55% identity). Both PPX and PPV were identified by low-stringency hybridization of mammalian cDNA libraries (12, 13), and their function is unknown. Recently, M. Yanagida's laboratory has shown that type 1 and type 2A phosphatases in *S. pombe* perform distinct functions (21). In this report, we show that the *S. cerevisiae* SIT4 phosphatase performs a unique function that cannot be performed by type 1 or type 2A PPases (in a *ssd1-d* background).

SIT4 functions in late G_1 for progression into S phase. At about the G_1/S transition, SIT4 associates in separate complexes with two high-molecular-weight proteins, p155 and p190. Therefore, the SIT4/p155 and the SIT4/p190 complexes may be the forms of SIT4 required in late G_1 for entry into S phase. One possibility is that p155 and p190 modify the substrate specificity of SIT4. Analogous to the high-molecular-weight subunits of mammalian type 1 PPases that target the phosphatase to specific substrates, p155 and p190 may target SIT4 to specific substrates at the G_1/S transition. Unfortunately, the proteins that SIT4 dephosphorylates at the G_1/S transition are not currently known. Also, it is not known if the G_1/S substrates of SIT4 include the transcriptional substrates of SIT4. In their complex with SIT4, both p155 and p190 are phosphorylated. Therefore, it is possible that the phosphorylation state of p155 and p190 controls their association with SIT4. When the 161-kDa glycogen-targeting subunit of rabbit skeletal muscle type 1 PPase is phosphorylated by cAMP-dependent protein kinase, it dissociates from the catalytic subunit (11). In an analogous fashion, perhaps the phosphorylation of p155 and p190 by cAMP-dependent protein kinases causes them to dissociate from SIT4 in early G_1. In late G_1, the reassociation of p155 and p190 with SIT4 could be regulated by the phosphorylation, at different residues, by another kinase (for example, CDC28). For this model, a PPase would be required to reset the system. Certain aspects of this model are readily testable.

ACKNOWLEDGMENTS

We thank M. Goebl for searching his personal collection of DNA sequences with the SSD1 sequence, M. Yanagida and K. Tatchell for sharing unpublished data on *dis3* and *SRK1*, L. Riles and M. Olsen for mapping *SSD1* and *PPH2α* to their yeast physical map, R. Derby and D. Spector for electron microscopy, B. Futcher for anti-CDC28 antibody, the B. Futcher and M. Wigler labs for strains and plasmids, W. Herr and F. Tanaka for 12CA5 ascites and peptide containing the epitope, and C. Devlin, B. Futcher, F. C. Lin, and M. Tyers for comments on the manuscript.

This research was supported by National Institutes of Health grant GM39892 to K.T.A.

REFERENCES

1. **Amati, B. B., and S. M. Gasser.** 1988. Chromosomal ARS and CEN elements bind specifically to the yeast nuclear scaffold. Cell **54**:967–978.
2. **Arion, D., L. Meyer, L. Brizuela, and D. Beach.** 1988. *cdc2* is a component of the M phase specific histone H1 kinase: evidence for identity with MPF. Cell **55**:371–378.
3. **Arndt, K. T., C. Styles, and G. R. Fink.** 1987. Multiple global regulators control *HIS4* transcription in yeast. Science **237**:874–880.
4. **Arndt, K. T., C. A. Styles, and G. R. Fink.** 1989. A suppressor of a *HIS4* transcriptional defect encodes a protein with homology to the catalytic subunit of protein phosphatases. Cell **56**:527–537.
5. **Axton, J. M., V. Dombradi, P. T. W. Cohen, and D. Glover.** 1990. One of the protein phosphatase I isozymes in Drosophila is essential for mitosis. Cell **63**:33–46.
6. **Beach, D. H., L. Rodgers, and J. Gould.** 1985. *RAN1*$^+$ controls the transition from mitotic division to meiosis in fission yeast. Curr. Genet. **10**:297–311.
7. **Blow, J. J., and P. Nurse.** 1990. A cdc2-like protein is involved in the initiation of DNA replication in Xenopus egg extracts. Cell **62**:855–862.
8. **Boeke, J. D., F. Lacroute, and G. R. Fink.** 1984. A positive selection for mutants lacking orotidine-5′ phosphate decarboxylase activity in yeast: 5-fluoro-orotic acid resistance. Mol. Gen. Genet. **197**:345–346.
9. **Booher, R., and D. Beach.** 1989. Involvement of a type I protein phosphatase encoded by *bws1*$^+$ in fission yeast mitotic control. Cell **57**:1009–1016.
10. **Carlson, M., and D. Botstein.** 1982. Two differentially regulated mRNAs with different 5′ ends encode secreted and intracellular forms of yeast invertase. Cell **28**:145–154.
11. **Cohen, P.** 1989. The structure and regulation of protein phosphatases. Annu. Rev. Biochem. **58**:453–508.
12. **Cohen, P., and P. T. W. Cohen.** 1989. Protein phosphatases come of age. J. Biol. Chem. **264**:21435–21438.
13. **Cohen, P. T. W., N. D. Brewis, V. Hughes, and D. J. Mann.** 1990. Protein serine/threonine phosphatases; an expanding family. FEBS Lett. **268**:355–359.
14. **Da Cruz e Silva, E. F., S. Alemany, D. G. Campbell, and P. T. W. Cohen.** 1987. Isolation and sequence analysis of a cDNA clone encoding the entire catalytic subunit of a type-2A protein phosphatase. FEBS Lett. **221**:415–422.
15. **Daniel, J., J. M. Becker, E. Enari, and A. Levitzki.** 1987. The activation of adenylate cyclase by guanyl nucleotides in *Saccharomyces cerevisiae* is controlled by the *CDC25* start gene product. Mol. Cell. Biol. **7**:3857–3861.
16. **Doonan, J. H., and N. R. Morris.** 1989. The *bimG* gene of Aspergillus nidulans, required for completion of anaphase, encodes a homolog of mammalian phosphoprotein phosphatase I. Cell **57**:987–996.
17. **Field, J., J. Nikawa, D. Broek, B. MacDonald, L. Rodgers, I. A. Wilson, R. A. Lerner, and M. Wigler.** 1988. Purification of a *RAS*-responsive adenylyl cyclase complex from *Saccharomyces cerevisiae* by use of an epitope addition method. Mol. Cell. Biol. **8**:2159–2165.
18. **Gautier, J., C. Norbury, M. Lohka, P. Nurse, and J. Maller.** 1988. Purified maturation-promoting factor contains the product of a Xenopus homolog of the fission yeast cell cycle control gene *cdc2*$^+$. Cell **54**:433–439.

18a. **Goebl, M.** Personal communication.

19. **Harlow, E., and D. Lane.** 1988. Antibodies: a laboratory manual. Cold Spring Harbor Laboratory, Cold Spring Harbor, N.Y.
20. **Kilmartin, J. V., and A. E. M. Adams.** 1984. Structural rearrangements of tubulin and actin during the cell cycle of the yeast *Saccharomyces*. J. Cell Biol. **98**:922–933.
21. **Kinoshita, N., H. Ohkura, and M. Yanagida.** 1990. Distinct, essential roles of type I and 2A protein phosphatases in the control of the fission yeast cell cycle. Cell **63**:405–415.
22. **Laemmli, U. K.** 1970. Cleavage of structure proteins during assembly of the head of bacteriophage T4. Nature (London) **227**:680–685.

22a. **Lin, F. C., and K. T. Arndt.** Unpublished results.

23. **Matsumoto, K., I. Uno, and T. Ishikawa.** 1985. Genetic analysis of the role of cAMP in yeast. Yeast **1**:15–24.
24. **Nagawa, F., and G. R. Fink.** 1985. The relationship between the "TATA" sequence and transcription initiation sites at the *HIS4* gene of *Saccharomyces cerevisiae*. Proc. Natl. Acad. Sci. USA **82**:8557–8561.
25. **Nash, R., G. Tokiwa, S. Anand, K. Erickson, and A. B. Futcher.** 1988. The WHI1$^+$ gene of *S. cerevisiae* tethers cell division to cell size and is a cyclin homolog. EMBO J. **7**:4335–4346.
26. **Ohkura, H., Y. Adachi, N. Kinoshita, T. Toda, and M. Yanagida.** 1988. Cold-sensitive and caffeine-supersensitive mutants

of the *Schizosaccharomyces pombe dis* genes implicated in sister chromatid separation during mitosis. EMBO J. **7**:1465–1473.

27. **Ohkura, H., N. Kinoshita, S. Miyatani, T. Toda, and M. Yanagida.** 1989. The fission yeast *dis2*$^+$ gene required for chromosome disjoining encodes one of two putative type 1 protein phosphatases. Cell **57**:997–1007.
28. **Reed, S.** 1980. The selection of S. cerevisiae mutants defective in the start event of cell division. Genetics **95**:561–577.

28a. **Riles, L., and M. Olsen.** Unpublished results.

29. **Rose, M. D., and G. R. Fink.** 1987. *KAR1*, a gene required for function of both intranuclear and extranuclear microtubules in yeast. Cell **48**:1047–1060.
30. **Rose, M. D., P. Novick, J. H. Thomas, D. Botstein, and G. R. Fink.** 1987. A *Saccharomyces cerevisiae* genomic plasmid bank based on a centromere-containing shuttle vector. Gene **60**:237–243.
31. **Sass, P., J. Field, J. Nikawa, T. Toda, and M. Wigler.** 1986. Cloning and characterization of the high-affinity cAMP phosphodiesterase of *Saccharomyces cerevisiae*. Proc. Natl. Acad. Sci. USA **83**:9303–9307.
32. **Silhavy, T. J., M. L. Berman, and L. W. Enquist.** 1984. Experiments with gene fusions. Cold Spring Harbor Laboratory, Cold Spring Harbor, N.Y.

32a. **Sutton, A., and K. T. Arndt.** Unpublished results.

33. **Thomas, B. J., and R. Rothstein.** 1989. Elevated recombination rates in transcriptionally active DNA. Cell **56**:619–630.
34. **Tice-Baldwin, K., G. R. Fink, and K. T. Arndt.** 1989. BAS1 has a Myb motif and activates *HIS4* transcription only in combination with BAS2. Science **246**:931–935.
35. **Toda, T., S. Cameron, P. Sass, and M. Wigler.** 1988. *SCH9*, a gene of *Saccharomyces cerevisiae* that encodes a protein distinct from, but structurally related to, cAMP-dependent protein kinase catalytic subunits. Genes Dev. **2**:517–527.
36. **Toda, T., S. Cameron, P. Sass, M. Zoller, J. D. Scott, B. McMullen, M. Hurwitz, E. G. Krebs, and M. Wigler.** 1987. Cloning and characterization of *BCY1*, a locus encoding a regulatory subunit of the cyclic AMP-dependent protein kinase in *Saccharomyces cerevisiae*. Mol. Cell Biol. **7**:1371–1377.
37. **Towbin, H., T. Staehelin, and J. Gordon.** 1979. Electrophoretic transfer of proteins from polyacrylamide gels to nitrocellulose sheets: procedure and some applications. Proc. Natl. Acad. Sci. USA **76**:4350–4354.

38. **Wilson, R., and K. Tatchell.** Personal communication.

39. **Wittenberg, C., and S. I. Reed.** 1988. Control of the yeast cell cycle is associated with assembly/disassembly of the cdc28 protein kinase complex. Cell **54**:1061–1072.
40. **Wittenberg, C., S. L. Richardson, and S. I. Reed.** 1987. Subcellular localization of a protein kinase required for cell cycle initiation in *Saccharomyces cerevisiae*: evidence for an association between the CDC28 gene product and the insoluble cytoplasmic matrix. J. Cell Biol. **105**:1527–1538.

41. **Yanagida, M.** Personal communication.